Performance and Sustainability Aspects of Fiber Reinforced Limestone Calcined Clay (LC3) Composites: A review

Sakib Hasnat*[a]

[a] *Department of Civil Engineering, Bangladesh University of Engineering & Technology, Dhaka, Bangladesh.*

Performance and Sustainability Aspects of Fiber Reinforced Limestone Calcined Clay (LC3) Composites: A review

Abstract

Concrete, a fundamental material in modern construction, has contributed significantly to global infrastructure development but is burdened by environmental concerns due to its high carbon footprint. This review paper explores Limestone Calcined Clay Cement (LC3) as an eco-friendly alternative, focusing on its blend with fibers to enhance mechanical properties while reducing environmental impact. LC3, a blend of limestone, clay, and gypsum, offers reduced CO_2 emissions compared to conventional cement. Various fibers, including polyethylene, polypropylene, polyvinyl alcohol, steel, and carbon fibers, have shown promising results in LC3 composites. The paper reviews mix proportions, fresh properties, mechanical performance, durability, microstructural characteristics, and environmental aspects of fiber-reinforced LC3 blends. Findings indicate that LC3-based composites exhibit high tensile strain, high toughness, reduced drying shrinkage, controlled crack propagation, and reduced CO_2 emissions, making them promising for sustainable construction. This review aims to provide insights into the properties and performance of fiber-reinforced LC3 blends, contributing to the development of environmentally friendly building materials with low carbon footprints. Further research in fiber reinforced LC3 composites should be focused on optimization of the mix design, fiber content and production process of LC3-fiber composites and understanding the microstructural behavior of the fiber-matrix interface and its effect on the mechanical properties.

1 Introduction

Throughout recent history, concrete has been instrumental in shaping modern society by facilitating the construction of many engineering marvels, residential buildings, dams, towering skyscrapers, expansive bridges and intricate road networks [1]. With the rise of rapid urban development across the globe and the ever-increasing need for infrastructure, cement has emerged as the most used material in the world, trailing only behind water [2]. Nevertheless, this development is coupled with environmental challenges, given that the production of Portland Cement can contribute significantly to global Carbon Dioxide (CO_2) emissions, accounting for nearly 5-7% of CO_2 emissions from human activities [3]. The resulting CO_2 emissions from Portland Cement can be around 0.66 to 0.82 kg-CO_2/kg of cement [4], [5]. Consequently, there is an increasingly shared view to reduce reliance on cement clinker to foster environmentally friendly construction practices, utilizing sustainable building materials [6].

Traditionally, Supplementary Cementitious Materials (SCMs) such as, fly-ash, slag, silica fume, metakaolin etc. have been used as eco-friendly replacements of cement, reducing the environmental impact of concrete production and enhancing its properties [7]. Recently, Limestone Calcined Clay Cement, which will be denoted as LC3 in this article from now on, has garnered attention as a solution to reduce clinker usage in the construction industry [8], [9]. The raw materials of LC3, limestone and clay, are both widely available in reserves around the world [10], [11]. It is common to replace half of the clinker in the cement-based composites with a mixture of calcined clay, limestone and gypsum in a ratio of 6:3:1. This mixture is typically known as LC3-50. The calcination of clay can be done at lower temperatures (600 to 800 °C) compared to cement production [12], transforming it to metakaolin. Metakaolin possesses beneficial pozzolanic characteristics and synergizes well with the limestone powder [12] in the formation of hydration products. The typical hydration product in LC3 blends is calcium-aluminate-silicate-hydrate (C-A-S-H), which is produced by the pozzolanic reaction of the alumina present in clay [13][14], [15]. Additionally, the calcium carbonate present in limestone reacts with the aluminates in the hydrated matrix to form mono and hemi-carboaluminate phases, which contribute to strength development [16]. Studies have shown that LC3 blended cementitious systems have shown similar or better compressive strength with replacement levels up to 50% and a more refined pore structure [17], however, increasing replacement levels can also result in delayed early strength development and reduced late age strength compared to Ordinary Portland Cement (OPC) blends [6]. Moreover,

LC3 replacement provides significant environmental benefits compared to conventional cement. Studies have revealed that LC3 can reduce around 20-35% of CO_2 emissions and around 22% of energy consumption compared to OPC [18], [19], [20]. The environmental benefits of clinker replacement, combined with satisfactory mechanical performance and pore refinement capability of the hydration products have made LC3 an emerging, and popular SCM with possible widespread applications in the future.

In order to improve the mechanical properties of concrete, the incorporation of fibers has become popular over the past half-century [21]. Fibers can improve the brittle fracture response of concrete, improve its low tensile resistance, and enhance the post-cracking toughness through controlled deformation and post-cracking response [22], [23]. The structural behavior of cementitious composites depends on both the strength and toughness. With regards to toughness, adding fibers to cementitious blends can impede the propagation of cracks, resulting in higher energy absorption capacity and improved toughness [24]. Moreover, fiber incorporated composites have also exhibited superior durability in terms of preventing shrinkage cracks and reducing permeability [25]. Engineering Cementitious Composites (ECC), also known as Strain Hardening Cementitious Composites (SHCC) [26] belongs to the general category of fiber-reinforced composites. ECC or SHCC has superior ultimate tensile strain and ultra-high ductility, generally ranging in two orders of magnitude higher than that of ordinary concrete, resulting in multiple cracking properties with the crack width generally controlled within 100 μm [27]. Fibers find their use in Ultra-high Performance Concrete (UHPC) as well, with steel fibers contributing to the excellent mechanical properties, toughness and pore characteristics of UHPC. However, both ECC and UHPC incorporate higher content of cementitious materials, with the cement dosage generally ranging around 1200 kg/m^3 for ECC, and 900-1100 kg/m^3 for UHPC. This excessive cement content raises considerable environmental concerns, as well as raising costs and causing drying shrinkage [28], [29]. Due to the usual low water-binder (w/b) ratio utilized in these systems, it is common to find most of the cement existing as filler material in these cementitious systems [30]. With the increasing demand for an environmentally friendly construction industry with a low carbon footprint, it is essential that cementitious binders with a low carbon footprint are utilized in ECC and UHPC, and general fiber-reinforced cementitious blends. In light of this, Limestone Calcined Clay Cement (LC3) based binders can offer considerable reduction in CO_2 emissions and satisfactory mechanical and durability properties. Various fibers have been utilized in LC3 blends

over the last few years, such as polyethylene (PE) [31], [32], polypropylene (PP) [33], polyvinyl alcohol (PVA) [34], [35], steel [36], [37], [38] and carbon fibers [39]. Researchers have also worked on 3d printed fiber reinforced concrete using LC3 binders [40], [41]. The incorporation of fibers in LC3 have resulted in improved early strength characteristics, tensile strain capacity, toughness and flexural strength. Furthermore, the durability characteristics of LC3 based cementitious systems can be improved with controlled autogenous cracks, in addition to reduced embodied energy and CO_2 emissions of LC3 [42].

Based on the engineering performance of fiber reinforced cementitious blends in terms of high tensile strain, crack control and ultra-high ductility, along with increasing concerns regarding eco-friendly building materials with low carbon footprint, a review is conducted in this paper on the properties and performances of fiber reinforced LC3 blends. The main purpose of the review is to aid researchers with the existing knowledge of fiber reinforced LC3 concrete and to pave the way forward for a more sustainable future for building materials. A thorough literature review was conducted using Scopus-indexed studies accessed through Google Scholar, applying the "Advanced search" feature to refine results. Key search terms included "LC3," "limestone calcined clay," "fiber," and specific fiber types such as "polyethylene fiber" and "polypropylene fiber" etc. to capture relevant studies. The subsequent sections of this paper present an in-depth analysis of the mix proportions, fresh-state properties, mechanical behavior, durability, microstructural characteristics, and environmental performance of fiber-reinforced LC3 blends. A scope of the review is presented in Fig. 1.

2 Summary of the Mix Proportions of Fiber Reinforced LC3 Blends

The studies reviewed incorporated a wide range of substitution levels of LC3 with cement. Furthermore, many of the studies utilized other pozzolanic material such as fly-ash and silica fume [35], [37], [43]. All of the studies reviewed have been published after 2020, which is due to the recent trend towards research into eco-friendly and sustainable materials for reducing the carbon footprint of the construction industry. Most of the studies reviewed incorporate a lower water-binder (w/b) ratio, and utilize the effect of high range water reducing admixture (HRWRA) or superplasticizers to aid in the development of sufficient workability. Researchers have utilized a wide range of synthetic fibers; however, no experimental studies have been found that analyze the effects of various natural fibers on the properties of LC3 blended cementitious mixes. Furthermore, there is a lack of studies that have utilized different fiber proportions in order to identify the effect

of various fiber replacements. Liu et al. [33], in their study used volume proportions of PP fibers ranging from 0% to 2.5% and observed that the 1.5% fiber replacement resulted in the lowest pore volume. Table 1 below presents a summary of the reviewed articles, in terms of mix proportions, aggregate used, fiber used and proportion of fiber, substitution ratios of LC3 and w/b ratio.

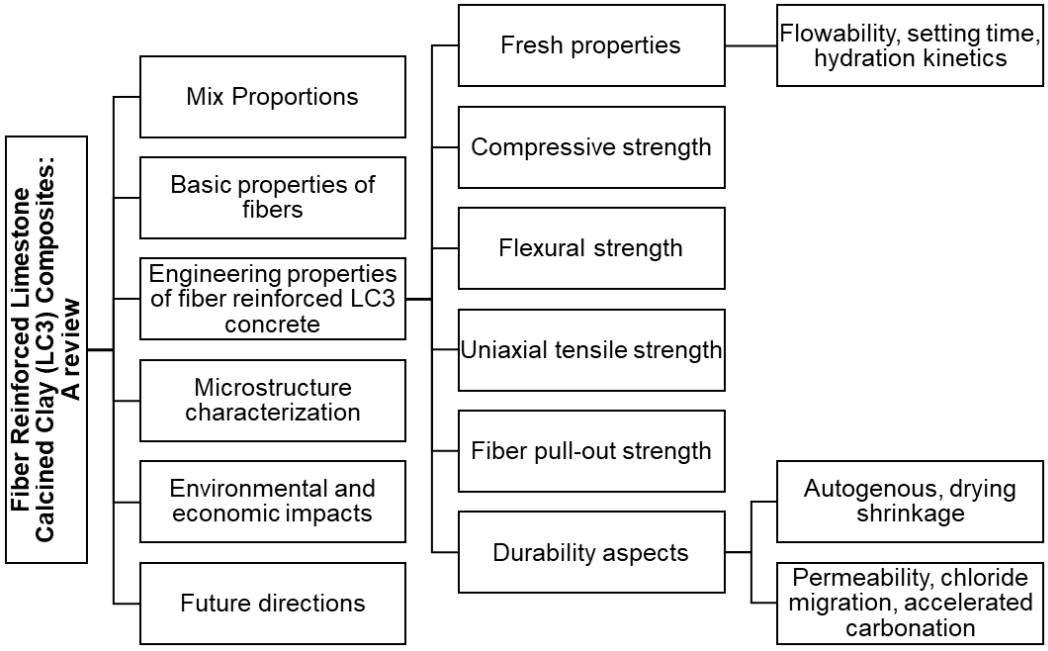

Figure 1. Outline of the review.

From Table 1, it can be seen that most of the studies utilize a w/b ratio in the range of 0.20 to 0.30 and with such low w/b ratios, the finer particles of LC3 take a larger specific surface area, requiring superplasticizers in almost all of the cases. Very few of the studies do not require any superplasticizer to achieve a desirable workability [33][34], [44]. Almost all of the studies use LC3 blends with calcined clay to limestone in the ratio of 2:1, nonetheless, some of the studies also explored the effect of different ratios of limestone to calcined clay [37], [45]. Researchers have analyzed the effects of LC3 replacement in a wide range, from 10% replacement to up to 80% LC3 replacement were found to be experimented with in the literature. Some of the studies also experimented with aggregates such as fly-ash cenosphere [28] and crumb rubber [46].

Table 1. Summary of mix proportions in fiber reinforced LC3 blends

Reference	Aggregate	Fiber	Fiber Percentage	LC3 Replacement	Calcined clay: Limestone	w/b ratio	Superplasticizer Used (y/n)
Zhou et al. [28]	Fly-ash cenosphere	PE	2% (vol.)	0% 35% 50% 65%	2:1	0.28	Y
Zhou et al. [47]	Sea sand RCA[a]	PE	N.A.	0% 35% 50%	2:1	0.39	Y
Gong et al. [31]	Sand	PE	N.A. (20 kg/m^3 of blended mix)	0% 35% 50%	2:1	0.25	Y
Wang et al. [32]	Sand	PE	2% (vol.)	0% 10% 30% 50%	2:1	0.204	Y
Mohammadi et al. [48]	Sand	PE	N.A.	70%	2:1	0.204	Y
Wang et al. [49]	Sand	PE	2% (vol.)	0% 50%	2:1	0.204	Y
Huang et al. [45]	Cenosphere	PE	0% 1% (vol.)	0% 45% 50% 65%	1:1 2:1 3:1	0.27	Y
Zhu et al. [50]	Sand	PP	2% (vol.)	45%	2:1	0.3 0.2 0.16	Y
Zhu et al. [51]	Sand	PP	2% (vol.)	14%	2:1	0.3	Y (0.7%, 0.8%, 0.9% of binder
Liu et al. [33]	N.A. (paste sample)	PP	0% 0.5% (vol.) 1% (vol.) 1.5% (vol.) 2% (vol.) 2.5% (vol.)	50%	2:1	0.4	N
Zhu et al. [46]	Sand Crumb Rubber	PP PE	1.5% (wt.) 1.3% (wt.)	0% 45%	2:1	0.25 0.3	Y
Zhang et al. [52]	Sand	PVA	2% (vol.)	0% 45% 45% (Coarse Limestone)	2:1	0.25-0.3	Y
Yu et al. [35]	Sand	PVA	2% (vol.)	70% 80%	2:1	0.3 0.35 0.4	Y
Chen et al. [34]	Sand	PVA	2% (vol.)	55% 70% 80%	2:1	0.3	N

Table 1. Continued.

Dong et al. [37]	Sand	Steel	2% (vol.)	0% 15% 20% 30% 40% 60%	2:1 1:1 1:2	0.18	Y
Luo et al. [43]	Sand	Steel	2% (vol.)	0% 20% 30% 40%	2:1	0.2	Y
Guo et al. [38]	Sand	Steel	2% (vol.)	0% 15% 30%	2:1	0.175	Y
Signorini et al. [44]	Sand	PBO[b]	N.A.	0% 75%	2:1	0.4	Y
Li et al. [39]	Sand	Carbon	1% (wt.)	0% 25% 50% 75%	2:1	0.5	N

[a]Recycled Concrete Aggregate, [b]Poly(p-phenylene-2,6-benzobisoxazole) (PBO) yarn.

3. Fibers Used in LC3 Mixes

3.1 Basic Parameters of Different Fibers

The basic properties of the fibers reviewed in this study are presented in Table 2. These basic parameters should be properly understood for the primary selection of fibers for experimental purposes. The mechanical properties of the fibers and size characteristics can influence the fiber-matrix bond and carry over to the macroscale properties of concrete. Elastic modulus, such a property, can influence the sensitivity of the fiber to hindrance of creep and shrinkage of the matrix and fibers with high aspect ratio are more sensitive to the improvements in tensile strength of the cementitious blend [53].

From the review of the studies, it can be easily understood that most of the studies experimenting with fiber reinforced LC3 cementitious mixes are focused on PE, PP, and PVA fibers and the manufacture of sustainable engineering cementitious composites (ECC) with ultra-high ductility and tensile strain capacity. Few of the studies also focused on producing sustainable ultra-high performance concrete (UHPC) with steel fibers. Although steel fiber is the most studied fiber, and the best one to strengthen concrete [54], it has not found extensive use in research utilizing LC3 concrete. Furthermore, basalt fiber, glass fibers are also commonly used to enhance the properties of concrete [54], have seen limited applications [55] with LC3 blends. Several eccentric fibers, such as Carbon fibers and Poly(p-phenylene-2,6-benzobisoxazole) (PBO) yarns have also been used in LC3 blends and exhibited satisfactory performances.

Table 2. Basic properties of fibers used in LC3 mixes.

Reference	Fiber	Length, mm	Diameter, µm	Tensile Strength, MPa	Elastic Modulus, GPa	Density, gm/cc	Melting Temperature, °C	Fineness, tex/dtex	Elongation, %
Zhou et al. [28]	PE	18	25	2900	116	0.97	150	-	-
Zhou et al. [47]	PE	12	25	2900	116	0.97			2.42%
Gong et al. [31]	PE	18	25	2900	116	0.97	150	-	-
Wang et al. [32]	PE	6	20	-	-	-	-	-	-
Mohammadi et al. [48]	PE	-	18	2500	80	0.97	-	-	3.5
Wang et al. [49]	PE	6	20	-	-	-	-	-	-
Huang et al. [45]	PE	12	24	3000	120	0.97	-	-	2.3
Zhu et al. [50]	PP	10	12	850	6	-	-	-	-
Zhu et al. [51]	PP	10	12	850	6	-	-	-	-
Liu et al. [33]	PP	12	25	630	7.1	-	-	-	-
Zhu et al. [46]	PP	10	12	850	6	0.91	-	-	21
	PE	12	24	2900	100	0.97	-	-	2.4
Zhang et al. [52]	PVA	8	39	1600	42.8	1.3	-	-	6
Yu et al. [35]	PVA	12	39	1600	42.8	1.3	-	-	-
Dong et al. [37]	Steel	13	200	-	-	7.85	-	-	-
Luo et al. [43]	Steel	13	200	2850	200	7.85	-	-	-
Guo et al. [38]	Steel	13	220	2850	-	7.8	-	-	-
Signorini et al. [44]	PBO	-	12	5800	270	1.56	650	1.7 dtex	25
Li et al. [39]	Carbon	0.53	7	4400	255	1.8	-	3420 tex	1.65

3.2 Different Types of Fibers

3.2.1 Polyethylene (PE) fiber

Polyethylene (PE) fibers are highly anisotropic structures characterized by high strength, high modulus, corrosion and weathering resistance. PE fibers have low surface energy and lack reactive groups, resulting in hydrophobic properties and weak adhesive properties [56]. PE fibers can sufficiently improve the ductility of concrete compared to other synthetic fibers [57], [58]. Researchers have also reported that PE fibers can result in tensile strain capacity up to 12%, which is even higher than some reinforcing alloys used in concrete [59], [60]. Zhou et al. [28], in their

research, observed that the hydrophobic nature of PE fiber limited the bridging between fiber and the cementitious matrix. Furthermore, low initial cracking stress due to LC3 replacement resulted in weakening the fiber matrix bond, resulting in the PE fiber being more prone to being pulled out. Nevertheless, the observed tensile strain capacity was higher than the control specimens without LC3 replacement.

3.2.2 Polypropylene (PP) fiber

Polypropylene (PP) fibers are cut, extruded and oriented polymer material which can be either straight or deformed. PP fibers can generally be subdivided into microfibers and macrofibers [61]. The length of macrofibers generally ranges between 30 and 50 mm, whereas, fibers shorter than 30 mm are characterized as microfibers. For the purpose of this review, microfibers are of greater importance due to their ability to limit the development of cracks and inhibit plastic shrinkage in concrete [62]. This results in enhanced durability of the structural element. Studies have shown that the incorporation of PP fiber in concrete can result in limiting crack formation [63], improving post-cracking behavior and toughness [64], enhanced tensile [65] and flexural strength [66]. Liu et al. [33] also reported that incorporation of PP fiber in LC3 cementitious mixes results in improved flexural strength by the fiber acting as a bridge to the matrix.

3.2.3 Polyvinyl Alcohol (PVA) fiber

Polyvinyl Alcohol (PVA) fibers incorporated into concrete result in improved flexural strength [67], crack and impact resistance [68], [69]. The existing research has found the incorporation of 0.5% to 1% fiber content is optimal, with the PVA fiber coordinating efficiently with concrete with respect to strain behavior. This is due to the similar elastic modulus of the two materials. Furthermore, hydrophilic groups on the fiber surface result in a rigid chemical bond between the PVA fiber and hydration products in the cementitious matrix [70]. PVA fibers incorporated in LC3 systems have shown that the relatively lower early matrix strength of LC3 reduced the stress needed for initiating new cracks, resulting in lower crack bridging capability compared to reference mixes without LC3 replacement [52].

3.2.4 Steel fiber

Steel fibers are short, discrete fibers having an aspect ratio ranging from 20-100, which have been used extensively for improving the properties of high performance concrete, both for structural and non-structural purposes [71]. Steel fibers enhance the stiffness, ductility, toughness, tensile

and flexural strength, as well as the compressive strength and torsional performances of concrete [72], [73], [74]. The steel fibers essentially "bridge" the cracks and improve the toughness of the cracked matrix, which results in improved shear bearing capacity and compression ductility of structural elements [70]. It is evident from the review conducted that, compared to traditional concrete, steel fibers have not yet been extensively used in high performance LC3 blends. In the research conducted by Guo et al. [38], it was observed that the average bond strength with the steel fiber increased up to 15% LC3 replacement, but it slightly reduced with higher replacement ratios.

3.2.5 PBO fiber

Poly(p-phenylene-2,6-benzobisoxazole) is a lightweight, high-stiffness, and high-strength woven textile material that has recently found its use in fiber reinforced concrete. PBO fibers are suitable for application in aggressive weathering conditions, high temperature and also under dynamic loading [75], [76]. PBO enhanced cementitious composites have been used for retrofitting purposes as well due to the improved ductility and stiffness [77]. However, the strong hydrophobic nature of PBO fibers prevents chemical interaction with the matrix, resulting in slippage and pullout failure dominant behavior in cementitious composites, resulting in the tensile strength potential of PBO remaining mostly untapped [78].

3.2.6 Carbon fiber

Carbon fibers are typically used as reinforcement in concrete in the form of short, multifilament segments about 10 mm in length. Similar to other synthetic fibers, incorporation of carbon fibers into cementitious systems results in improved flexure and ductility, fatigue performance, longevity and strength [79], [80], [81]. However, carbon fibers are more effective in improving the toughness and post-cracking response in concrete compared to improvements in compressive strength [70]. Furthermore, the high cost and electrical sensitivity of carbon fibers also present a drawback in its used in concrete [82]. There have been very limited studies in the field of LC3 cementitious blends that explore the influence of carbon fibers on the fiber-matrix behavior and mechanical properties of LC3 concrete [39].

4 Engineering Properties of Fiber Reinforced LC3 Blends

In order to evaluate the mechanical and durability properties of the fiber reinforced LC3 mixes, scholars performed a wide range of tests. The tests found from the reviewed literature are testing for workability, initial/final setting time, hydration kinetics, compressive strength, three point

bending, splitting tensile strength, uniaxial tensile, fiber pull-out, cracking response, drying shrinkage, autogenous shrinkage, permeability, chloride migration, carbonation etc. However, not all the studies performed all of the tests.

4.1 Fresh Properties

4.1.1 Flowability and Setting Time

Researchers measured the workability of the fresh LC3 paste mixed with different using standards such as BS EN 4551, Chinese standard GB/T 2419-2005, GB/50119-2013, ASTM C230, ASTM C1437. Most of the tests are popularly known as flow table tests. The setting times (initial/final) are measured in accordance with ASTM standard C807. The flowability of LC3 blended fiber composites from the studies reviewed for different fiber types and mix designs have been presented in Fig. 2. Due to the high specific surface area of the LC3, it was observed that the workability reduced with increasing LC3 replacement. Li et al. [39] observed that the spread diameter in the flow table test decreased drastically with increasing LC3 content. 75% LC3 replacement resulted in a 257% increase in the specific surface area, resulting in the flow table diameter decreasing from 250 mm to only 90 mm. This property of LC3 required the usage of High Range Water Reducing Admixture (HRWRA) or superplasticizers to achieve workability similar to that of cementitious mixes with no LC3 replacement.

The decrease in workability with increasing LC3 content was observed irrespective of fiber replacement content. Zhou et al. [28] incorporated 2% PE fibers into the LC3 matrix and observed that the flowability reduced with increasing LC3 content, with a 19% reduction in the flow diameter value for 65% LC3 replacement. Wang et al. [32], in their study observed very similar workability with the control mix due to use of superplasticizers and slightly increasing the water content. They were able to achieve 192 mm flow diameter at 0.204 w/b ratio, which is more than the flow diameter of the control specimen of 187 mm. Gong et al. [31] observed a 5% decrease in flowability with 50% LC3 replacement. Zhu et al. [51] used PP fibers combined with LC3 to develop sprayable engineered cementitious composites (ECC). The researchers used a deformability index defined as,

$$D = \frac{(d_1 \times d_2) - {d_0}^2}{{d_0}^2} \quad (1)$$

Where d_1 is the maximum spread diameter, d_2 is the diameter measured perpendicular to d_1 and d_0=10 cm for the equipment used. The authors observed that the deformability index rapidly decreased with time due to the buildup of rapid hardening calcium sulfo-aluminate (CSA) cement used. A maximum deformability index of 2.5 was proposed for sprayable ECC thickness buildup without dripping and an index of 1.8 was preferred for good atomization quality of ECC at the spray nozzle. One study done by Liu et al. [33] experimented with PP fiber contents ranging from 0% to 2.5%, and it was observed the increase in fiber content resulted in decreased workability (Fig. 2). Using 180 mm as the normative value, it was observed that the working requirements are met at 1% fiber content. Researchers using PVA fibers as reinforcement generally controlled the spread diameter to within 160-230 mm by using superplasticizers in suitable amounts [35], [52]. Guo et al. [38] incorporated steel fibers with LC3 and nano-silica (0%, 1%, 2%) to produce UHPC and observed that the fluidity reduced with increasing nano-SiO_2 replacement, owing to the high specific surface area of nano-SiO_2. The density of ECC using PE fibers was found to range around 1412-1460 kg/m^3 and those using PVA fibers were found to range around 1900-2100 kg/m^3 [28], [35].

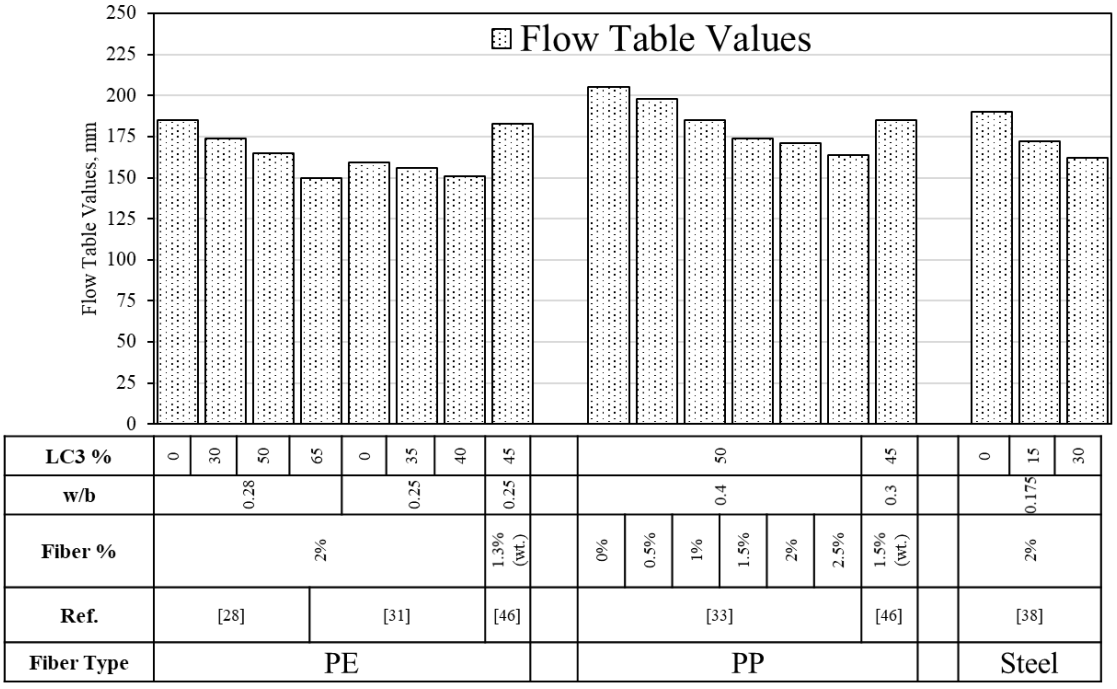

Figure 2: Flow table values of fiber reinforced LC3 for varying LC3 replacement, w/b ratio and fiber percentage.

It was generally observed that the setting time, both initial and final setting time reduced with increasing LC3 replacement. This could be attributed to the higher specific surface area of calcined clay reducing the amount of free water in the matrix, combined with the gypsum present in LC3 blends affecting the setting time. At higher replacement levels, the slow pozzolanic reaction of calcined clay could delay the setting time slightly [32]. Li et al. [39] observed the setting time reducing from 7 hours to only 1.2 hours with 75% LC3 replacement.

4.1.2 Hydration Kinetics

The hydration kinetics of fresh pastes incorporating LC3 substitution was evaluated by researchers using isothermal calorimeters up to 72 hours and it was observed that inclusion of LC3 into the cementitious blends resulted in a reduction in the cumulative heat of hydration [32], [45]. This was prominently due to the reduced clinker content and reduced C_3S, resulting in a dilution effect [83]. Substitution of LC3 resulted in a slightly quicker time to reach the hydration peak, resulting in the workability of the composites slightly decreasing with increasing LC3 substitution [39]. From the heat release curves of LC3 based composites, two distinct peaks can be observed (Fig. 3), the first of which corresponds to the hydration of silicates, namely C_3S and the second peak corresponds to aluminates [84]. It was observed that the first peak was reached earlier for LC3 composites due to the filler effect of calcined clay and its high specific surface area. As a result, the hydration of LC3 blends is accelerated and the aluminate peak is heightened. Dong et al. [37] observed the distinct second aluminate peak only for high substitution levels. The researchers observed a decrease in the peak height and an increase in width due to the reaction of calcined clay competing with that of the clinker hydration, resulting in a higher cumulative heat release for higher calcined clay:limestone ratios. Broad humps in the heat flow curve in LC3 blended composites have been observed during the first hour due to the slow dissolution of gypsum [85] and the rapid generation of ettringite due to the reaction of C_3A with calcium sulfate [86]. After the first hour, the CH gets consumed and early C-A-S-H is formed, resulting in reduced workability [85]. Li et al. [39] also noted that increasing the LC3 replacement resulted in the curve shifting toward the left due to the nucleation effect of limestone and calcined clay particles.

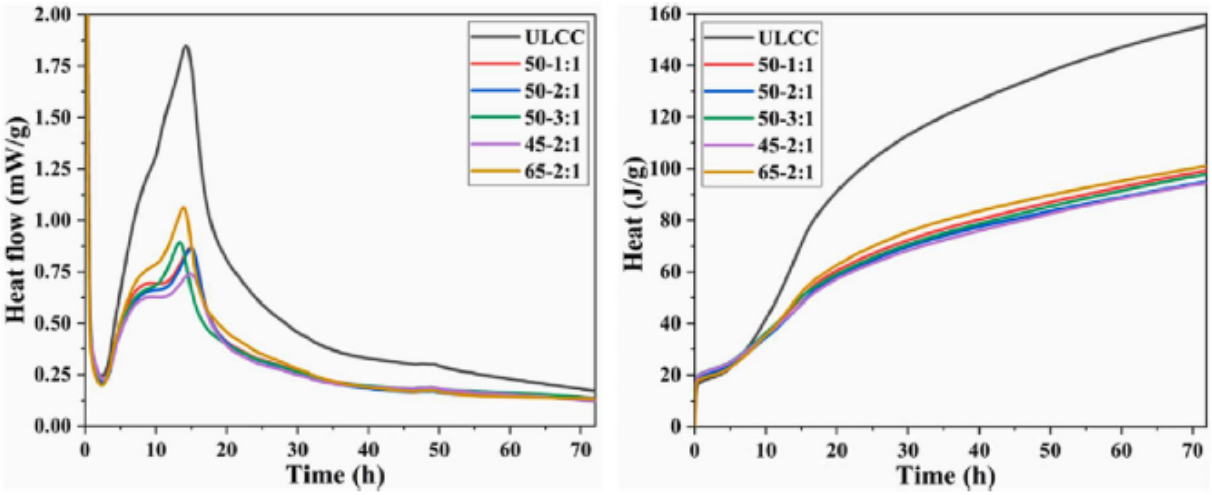

Figure 3. Results of isothermal calorimetry tests on LC3 blended composites, adapted from Ref. [45]. *ULCC refers to the mix without any LC3 replacement, 50-2:1 indicates 50% LC3 replacement with a calcined clay:limestone ratio 2:1

4.2 Compressive Strength

A summary of the compressive strengths obtained with different fiber ratios, LC3 replacements and w/b ratios are presented in Fig. 4. The findings show varying, somewhat contradicting effect of LC3 and fiber replacements on the early and late age strengths. For the incorporation of polyethylene (PE) fiber into LC3 replacement, Zhou et al. [28] noted a reduction in strength with increasing LC3 replacement for both early age and late age strengths. Conversely, Gong et al. [31] found higher early strength with 35% replacement, and attributed it to the high pozzolanic activity of calcined clay. Although the authors observed a slight reduction in strength at higher replacement, this is due to the dilution effect worsening as the cement replacement increases. From Fig. 4, Wang et al. [32]observed the highest strengths among other mixes with PP fibers, which is due to the incorporation of silica fume (SF) as a binder replacement, producing high strength mixes. The researchers observed slight decreases in strength at 10% and 30% replacement; however, a significant decrease in strength was observed at 50% replacement due to the portion of increased macro pores and low hydrate content in the LC3 matrix. The low clinker content, resulting in less portlandite (CH) being produced, also contributes to the reduced pozzolanic reaction and lower strength. LC3 replacement requires more water to attain similar levels of workability [52]. Similar results are observed by PVA fiber reinforced LC3 blends as well [34], [35], [87], as seen from Fig. 4. Li et al. [39] shed some light on this behavior. The authors stated that increased total pore volume and formation of ettringite due to LC3 replacement lead to

cracking in the hardened matrix. The same authors experimented with carbon fiber (CF) addition [39], and observed that although CF can enhance the performance of Portland Cement, it had a less pronounced or even negative effect on the LC3 blended matrix due to considerably weaker fiber bridging effect LC3 blends and lower bond strength.

Conversely, Huang et al. [45] observed an increase in the 28-day strength development, owing to the delayed strength development resulting from the pozzolanic reaction of reactive silica and alumina in calcined clay with the portlandite (CH) from the clinker. Inclusion of fibers in the blend can result in increased air content and porosity [46], [88], this resulted in slightly lower strength development. This is further confirmed by [33], who noted a decrease in compressive strength with increasing fiber volume due to air voids in the gel matrix, although the bonding effects between the fiber and the matrix can enhance the strength at earlier ages. Huang et al. [45] also observed a notable increase in the elastic modulus upon the addition of PE fiber. PE fiber reinforced cementitious layer has also been observed to strengthen the interfacial transition zone (ITZ) between recycled aggregates and the new mortar matrix, resulting in improved load transfer and controlling crack propagation [47].

As it can be seen from Fig. 4, utilizing steel fibers at just 2% volume resulted in considerably higher strengths than the other fibers reviewed. From [37], it was observed that LC3 replacement up to 31% resulted in increased strength with finer limestone resulted in higher strength. The authors experimented with different replacement levels of calcined clay and limestone and it was observed that increasing limestone content to greater than 20% resulted in a decrease of strength, whereas calcined clay replacements at levels more than 20% resulted in increased strength. Luo et al. [43] observed higher early strength with LC3 systems of more than 7.07% and 4.82% than the reference mix for 20% and 30% LC3 substitution, however, the 28 day strengths were all lower than the reference mix. This was explained by the early strength enhancement of LC3 systems due to quick pozzolanic reaction of calcined clay with portlandite (CH) to form denser hydration products of calcium alumino-silicate hydrate (C-A-S-H) gel. This rapid hydration occurred due to the synergistic interaction between the SF and LC3 blends. Similar to the study done by [37], Guo et al. [38] observed an increase in compressive strength with replacement levels up to 30% LC3.

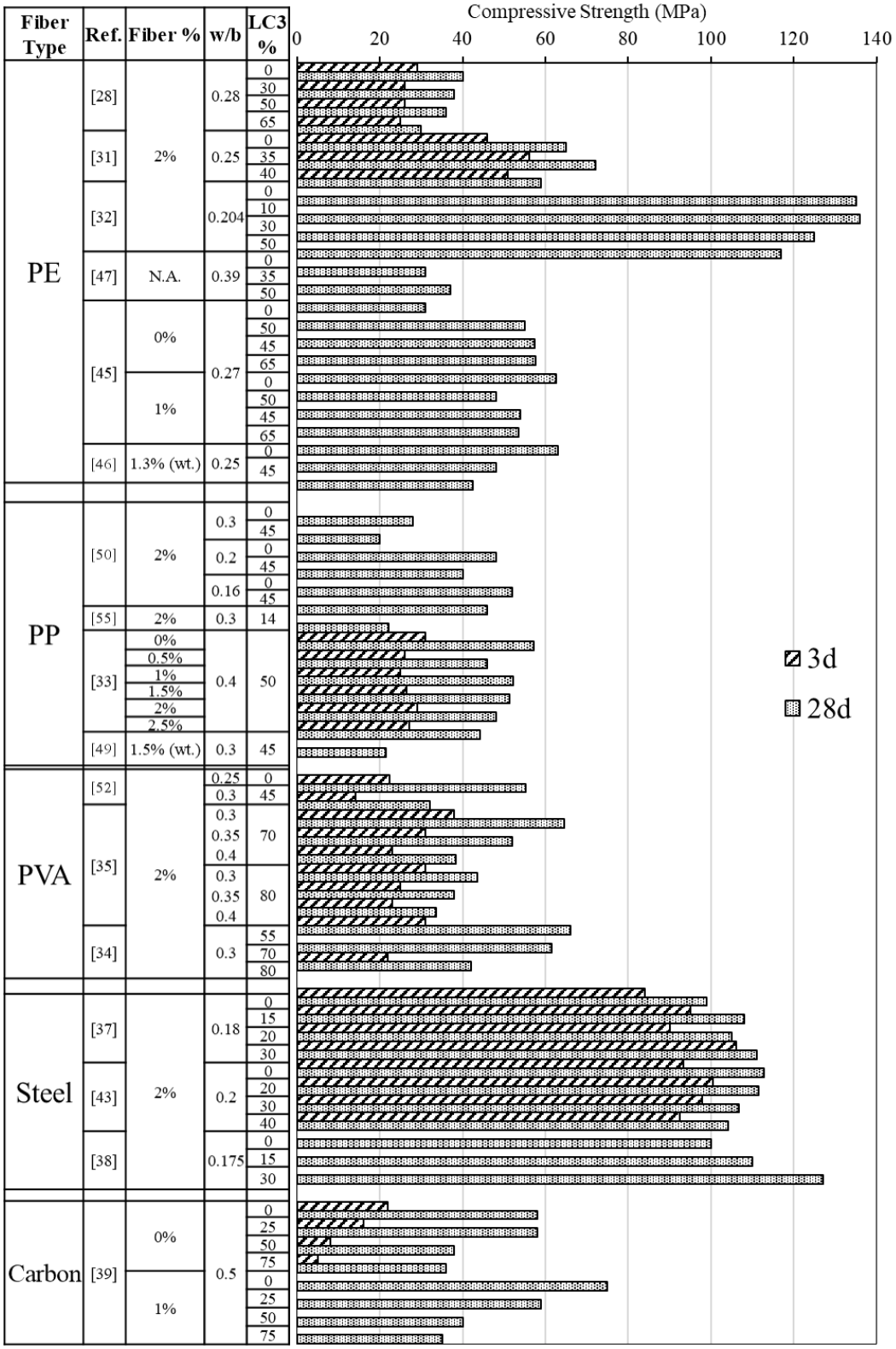

Figure 4. Compressive strength of fiber reinforced LC3 at 3-days and 28-days for varying LC3 replacement, w/b ratio and fiber percentage.

4.3 Flexural Strength

The effect of fiber reinforcement on the flexural strength of LC3 cementitious blends were evaluated for different types of fibers, LC3 replacement ratios, w/b ratio and fiber percentage. A summary of a few of the reported flexural strengths has been presented in Fig. 5. All of the flexural strength tests were conducted on 40 x 40 x 160 mm3 samples using either three-point or four-point bending tests. As it can be seen from Fig. 5, only 2% inclusion of PE fibers resulted in more than double the flexural strength of cementitious composites [32]. The same study noted that 10% LC3 replacement resulted in a more prominent increase in flexural strength compared to higher replacement ratios due to the relatively higher porosity of matrices with a high LC3 content. Ibrahim et al. [41] observed the presence of fibers in the macropores, resulting in improved mechanical performance. The increase in flexural toughness with LC3 replacement could be attributed to the formation of highly polymerized C-A-S-H gel and ettringite formation [89]. However, the authors in [32] observed that the fiber-matrix interface in the reference matrix had surface damage due to extensive pullout in the deflection-softening regime and hydration products (Fig. 6), indicating a stronger bond due to the denser C-A-S-H [90]. Hence, the stronger mechanical anchorage of PE fibers in the reference matrix is not truly representative of the macro-scale flexural performance of the LC3 blends.

Another study done by Wang et al. [49], revealed that the flexural strength of PE reinforced LC3 composites increased with exposure to freeze-thaw cycles and decreased for exposure to wet-dry cycles. Zhou et al. [28] developed a sprayable ECC utilizing PP fiber and experimented with its efficacy and bond behavior with regular concrete. Four-point bending tests were conducted on layered ECC and concrete specimens (Fig. 7), positioning the PP fiber reinforced ECC on the tension side of the beam. It was found that the specimen exhibited excellent strain-hardening properties, with the ultimate flexural strength of sprayed and cast ECC increasing to 5.6 and 5.9 MPa. Interestingly, no deliberate roughening was done along the interface, fostering moderate bonding and leading to more microcracks in the ECC, which in turn contributed to its ductile behavior.

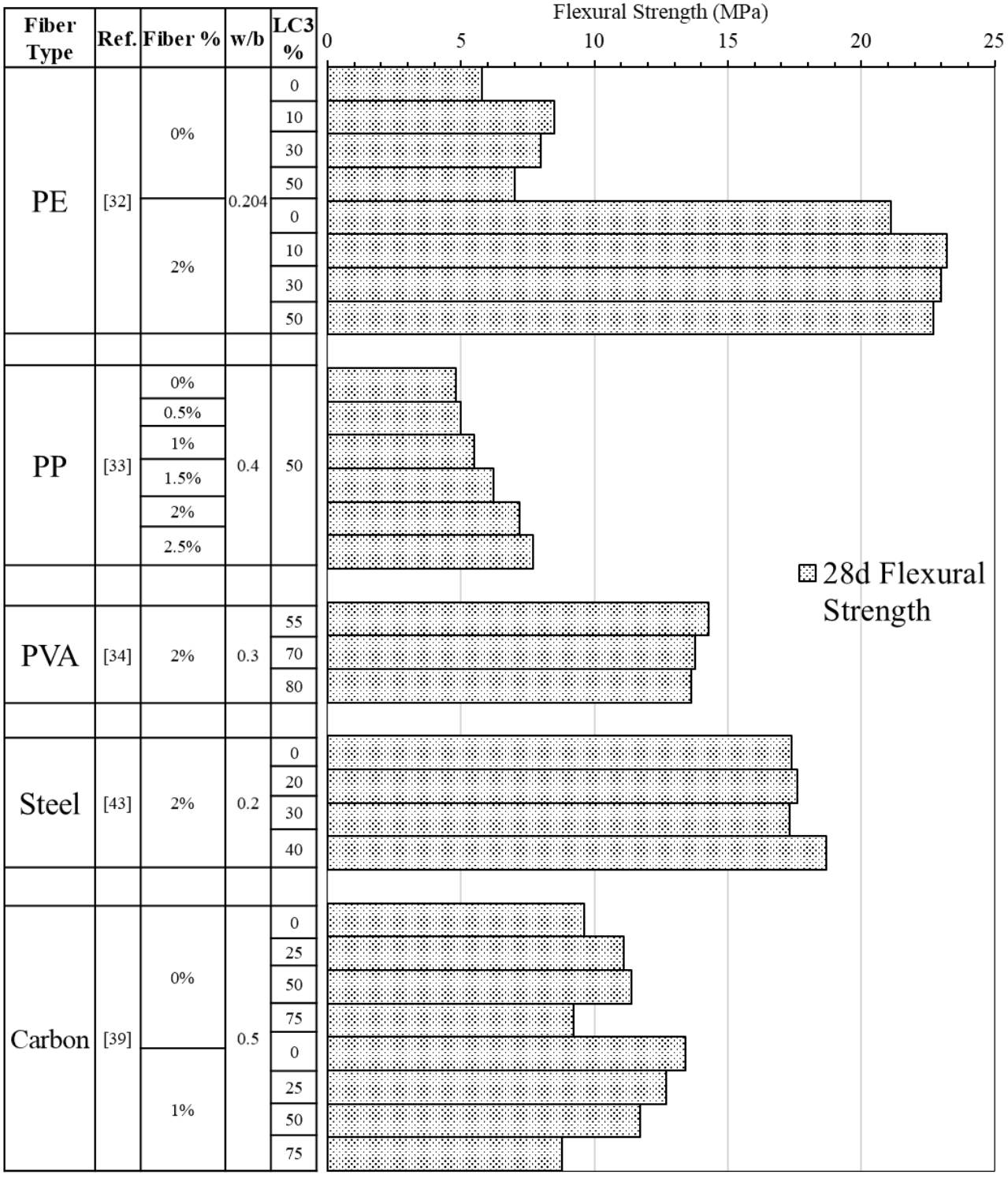

Figure 5. Flexural strength of fiber reinforced LC3 at 28 days for varying LC3 replacement, w/b ratio and fiber percentage.

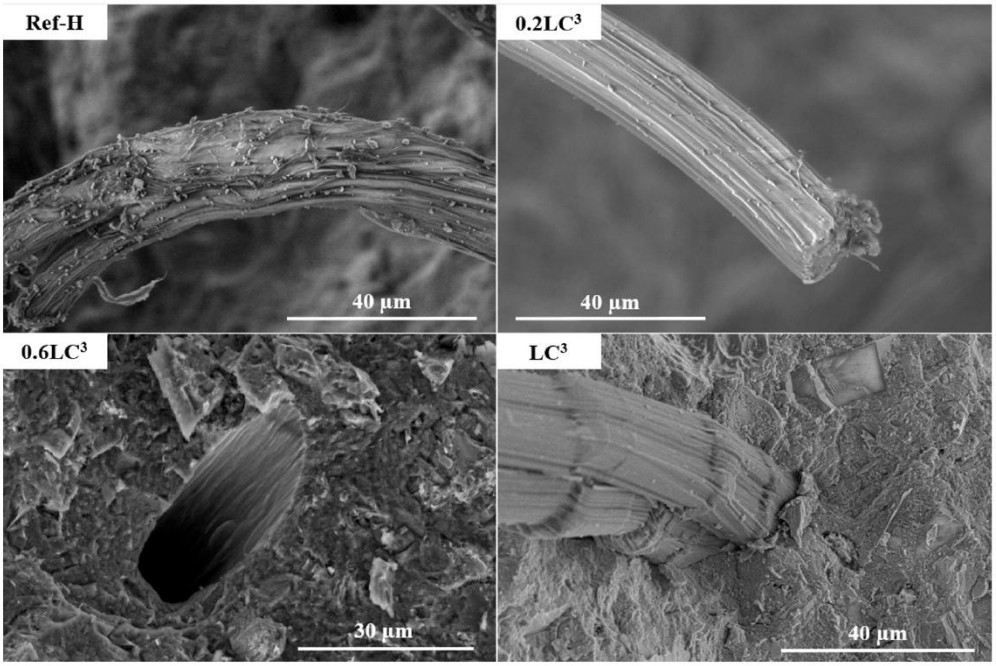

Figure 6. ESEM images showing the state of the fibers on the fracture surfaces of PE fiber reinforced LC3 specimens, adapted from Ref. [32].

Figure 7. Crack patterns of ECC-concrete composite under flexural loading, adapted from Ref. [51].

Liu et al. [33] and Zhu et al. [46] both investigated the influence of PP fibers on the flexural strength of LC3 blends. From Fig. 5, it can be observed that increasing fiber dosage resulted in increasing flexural strength, attributed to the bridging effect of fibers and the fiber toughening effect of the fiber-matrix composite [91]. Chen et al. [34] found that the flexural load-bearing capacity increased with higher LC3 replacement, while the energy absorption capacity decreased with LC3 replacement in PVA fiber reinforced ECC. Using steel fibers, Luo et al. [43] found lower earlier flexural strength in LC3 systems but a gradual increase after 28 days, with higher strength at higher replacement levels (Fig. 5). Researchers Li et al. [39] observed 20% flexural strength enhancement up to 50% LC3 replacement, attributed to hexagonal rod-shaped ettringite formation and highly polymerized C-A-S-H gel. The authors additionally noted that the incorporation of

carbon fibers resulted in a 17% increase in the flexural strength of 25% LC3 replacement. However, the enhancing effect of carbon fibers gradually decreased with increasing LC3 content, as corroborated by pullout tests.

4.4 Uniaxial Tensile Strength

In all of the studies reviewed, the researchers evaluated the tensile characteristics of fiber reinforced LC3 matrices using dog-bone shaped specimens in accordance with the recommendations of the Japan Society of Civil Engineers (JSCE) [92]. In general, the tensile load was applied at a rate of 1 mm/min and the deformation was measured over a gauge length of 80 mm. The schematic of the specimen is shown in Fig. 8.

A summary of the tensile strength results in terms of the ultimate tensile strength at failure and the tensile strain capacity with respect to varying LC3 replacements, fiber replacements, w/b ratio is presented in Fig. 9. From the figure, it is evident that although the ultimate tensile strength may or may not increase with increasing LC3 replacement, the tensile strain capacity improves considerably with incorporation of higher LC3 content. Additionally, PE fibers generally exhibit greater strain capacity compared to the other fibers; however, almost all of the points fall within the 4-6% range of strain capacity. Zhou et al. [28] found that PE fiber incorporation led to a higher tensile strain capacity compared to control specimens, despite lower initial cracking stress and ultimate stress attributed to LC3 replacement weakening the fiber-matrix bond. The hydrophobic nature of the PE fiber limited the bridging between fiber and matrix, resulting in the fiber being more prone to pull-out failure. Gong et al. [31] observed strain hardening behavior in LC3-based binders with PE fiber, with cracking stress increasing at 35% replacement but decreasing at 50%, influencing crack development and favoring controlled crack growth. Due to the controlled crack growth and prevention of brittle failure, the resulting strain capacity is the highest at 50% LC3 replacement. The beneficial effect of LC3 in enhancing strain energy absorption capacity has been confirmed by other researchers as well [45], [46]. This could be attributed to the lowering of the initial cracking stress of the matrix, which results in a controlled growth of cracks, preventing brittle failure [52] in addition to the pore refinement caused by the development of C-A-S-H gel in the matrices [45]. Zhu et al. [46] experimented with crumb rubber and observed that the crack width in LC3 blends was significantly reduced by the addition of crumb rubber due to an increase in the number of induced cracks.

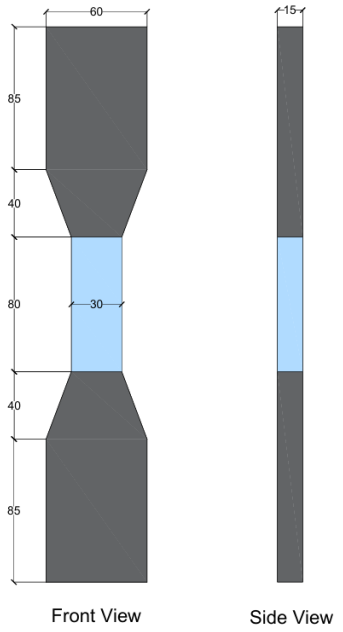

Figure 8. Dog-bone specimen for uniaxial tensile strength test.

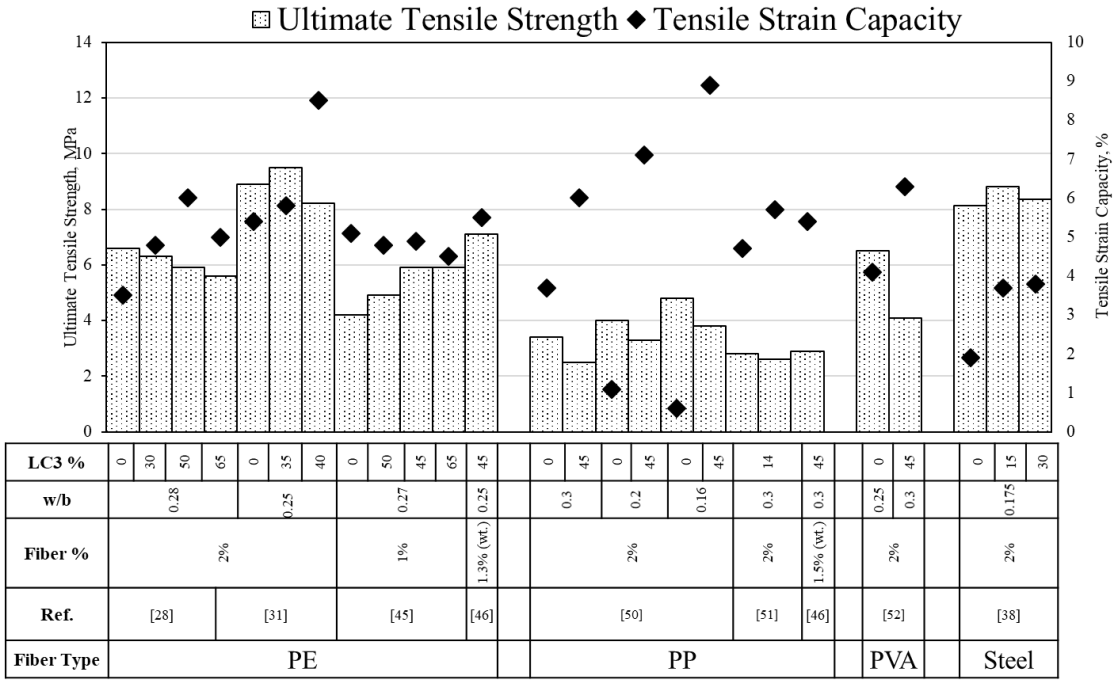

Figure 9. Ultimate tensile strength and tensile strain capacity fiber reinforced LC3 at 28 days for varying LC3 replacement, w/b ratio and fiber percentage.

Zhu et al. [50] reported a significant increase in tensile strain capacity, from 0.6% to 8.9% by 45% LC3 replacement, while the ultimate tensile strain values were comparable with traditional ECC. The authors [50] observed a tighter crack distribution with the LC3 concrete, signifying enhanced service lives of structures. As described previously, sprayable PP fiber reinforced LC3 developed by Zhu et al. [51] exhibited lower ultimate tensile strength and first cracking strength

than it's cast-in-place counterpart. Nonetheless, the strain capacity increased up to 5.7% for sprayable ECC, generating more controlled cracks with reduced width. The PP fiber reinforced composites exhibited superior ductility and crack control compared to PVA fiber reinforced ECC, despite the inferior mechanical properties of PP fibers [93]. Zhang et al. [52] observed that LC3 replacement increased first cracking stress and ultimate strength at earlier ages, which, however reduced at later ages. In line with the findings from other researchers, the authors also showed that LC3 blended mixes could exhibit more than 500-600 times the tensile strain capacity of traditional concrete. However, the researchers observed a larger crack width for LC3 replacement, contradicting the findings from Gong et al. [31] and Zhou et al. [28]. This could be due to the differences in the fiber-matrix interaction between PE fibers and PVA fibers, or the coarser limestone used in the Zhang et al. [52] study. Yu et al. [35] observed a decrease in tensile strength with increasing LC3 content and water/binder ratio, but higher tensile strain capacities in mixes with lower sand/binder ratios.

In steel fiber-reinforced ultra-high performance concrete (UHPC), Guo et al. [38] found that nano-SiO_2 additions improved tensile strength and strain, with LC3 replacement enhancing strain capacity but slightly reducing tensile strength increments. This is due to the relatively high reactivity of nano-SiO_2, contributing to the hydration reactions and resulting in the formation of a denser microstructure and improved fiber-matrix bond. It was observed that the tensile strain energy increased with LC3 replacement up to 15% replacement, but reduced slightly with further increments. Nonetheless, agreeing with the findings from other studies, the tensile strain capacity was enhanced considerably with increasing LC3 replacement.

The higher tensile strain capacity and ductility of LC3 blended mixes could be explained by the results of the single crack test performed on notched dog-bone specimens by Zhou et al. [28] and Zhang et al. [52]. It was observed that the reference mix had higher crack bridging capability due to the stronger interfacial transition zone (ITZ) of the fiber-matrix interface. As such, the lower matrix strength of LC3 mixes facilitated the formation of strain-hardening composites with much higher tensile strain capacity and lower crack widths of less than 100 μm [94]. Furthermore, the findings from the study done by Gong et al. [31] show that the calcined clay components essentially behave as thixotropic additives and, combined with the action of the water-

reducing admixture, the rheology properties of the paste are improved [95]. This results in a more uniform fiber dispersion, causing the tensile ductility of LC3 blended composites to increase.

4.5 Fiber pull-out strength

From the review conducted, it was apparent that there were no unified standards for conducting the fiber pull-out tests. Researchers have used setups with a fiber embedment length of 6 mm into the matrix with a free length of 1 mm, attaching the free end to a smooth aluminum plate using adhesive materials [28], [31]. A similar test setup with 5 mm embedment length has been used by Guo et al. [38] into their investigation of the fiber-matrix bond for steel fibers. Mohammadi et al. [48] investigated the effect of Dopamine and Tannic Acid treatment on the fiber-matrix bond by testing individual PE fibers of 20 mm length, gluing the fibers to paper, cardboard, and obtaining a 2 mm free length of fiber. A similar test setup was followed by Li et al. [39] for their experiments on virgin and recycled carbon fibers. Signorini et al. [44] used double sided pull-out tests on PBO yarns as adapted from Butler et al. [96]. A schematic illustration of the single fiber pull-out test setup has been presented in Fig. 10. The fiber bond strength from single fiber pull-out tests could be evaluated from equation (2) [97]. Where F_{max} is the recorded pullout force, d_f is the fiber diameter, L_e is the embedded length of the fiber.

$$\tau_0 = \frac{F_{max}}{\pi d_f L_e} \tag{2}$$

Zhou et al. [28] observed a hardening stage before fiber displacement with PE fibers, attributed to the hydrophobic nature of PE fiber and the subsequent negligible chemical bond between the matrix and the fiber. The bond strength reduced from 0.65 MPa to 0.51 MPa with 65% LC3 replacement, correlating with the descending tensile strengths and increasing tensile capacity with increasing LC3 replacement. However, this behavior was not consistent with the findings from other studies. Gong et al. [31] reported a maximum bond strength of PE fibers at 35% LC3 replacement of 0.63 MPa, and Wang et al. [32] also reported maximum bond strength of 0.65 MPa at 10% LC3 replacement. This behavior was explained by the weaker fiber-matrix bond for the reference matrix due to the higher micro-porosity of the matrix and confirmed by Mercury Intrusion Porosimetry (MIP) measurements. However, the thermodynamically driven fiber-matrix interactions of hydrophobic PE fibers could not be explained properly.

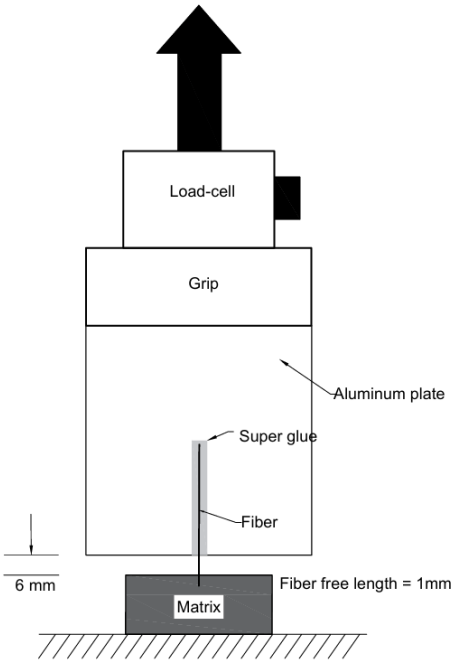

Figure 10. Schematic illustration of the single fiber pull-out test setup, adapted from Ref. [28].

Mohammadi et al. [48], in their study, successfully improved the fiber-matrix bond of hydrophobic PE fibers in LC3 matrices by surface modification using Dopamine (DA) and Tannic Acid (TA). A maximum pullout load of 0.1418 N was observed for a DA/TA ratio of 70/30, compared to 0.0391 N for untreated PE fiber. The higher tensile strength could be attributed to the activation of the PE fiber surface through a polymeric layer of DA/TA containing hydroxyl and amine groups, which form chemical bonds in the fiber-matrix interface [98]. Microscopic images of pulled out untreated PE fibers and 70/30-DA/TA treated fibers show the presence of cementitious matrix on the treated fibers, indicating a stronger adhesion strength and improvement of the fiber-matrix interfacial bond (Fig. 11). Signorini et al. [44] used a cementitious slurry to impregnate PBO yarns and improve their bond performance in LC3 systems. It was found that the impregnated PBO yarns exhibited a significant increase in bond strength and stiffness with impregnation, albeit at the partial cost of ductility compared to the untreated fibers. The treated fibers resulted in a 50% gain in ultimate stress over the untreated fibers.

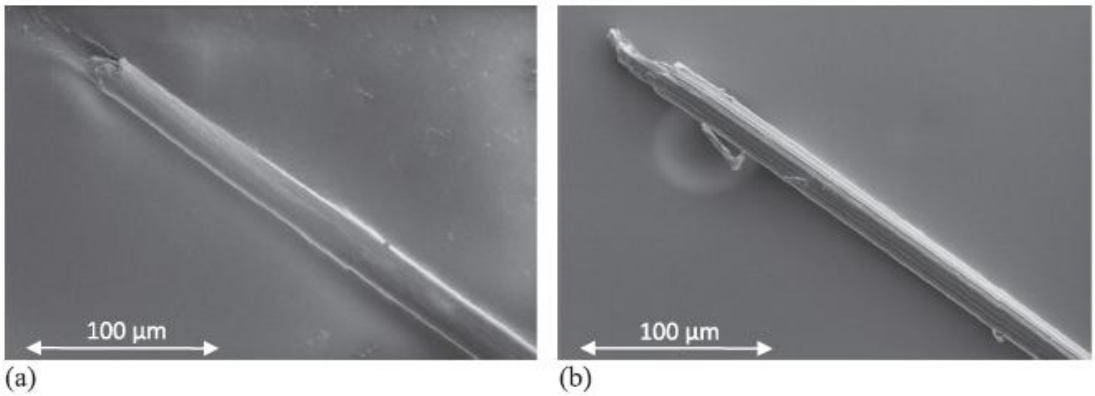

Figure 11. Microscopic images of (a) Untreated and (b) Treated PE fibers with DA/TA-70/30 after pullout testing, adapted from Ref. [48].

The average bond strengths for steel fibers subject to single fiber pull-out tests were significantly more than those with PE fibers. Guo et al. [38] reported the bond strength to increase slightly for 15% LC3 replacement to 10.97 MPa, which further reduced to 8.9 MPa with further replacement. For both PE and steel fibers, the bond strengths varying with LC3 replacements were found to correspond to their ultimate tensile strengths. The authors additionally reported that increasing nano-SiO_2 up to 2% proved to be excellent in improving the bond strength of steel fibers in LC3 matrices. Conversely, [39] found poor bond performance between carbon fibers and the cementitious matrix with increasing LC3 content, attributed to enhanced expansion, resulting in a higher diameter of the hole in which the fiber is embedded, resulting in reduced confinement pressure. The presence of more ettringite crystals at the fiber-mortar interface resulted in reduced bond strength with increasing LC3 replacement. Thus, the behavior of different fibers at the fiber-matrix interface with varying LC3 content should be further looked into in future studies.

4.6 Durability Aspects

4.6.1 Autogenous and Drying Shrinkage

The autogenous shrinkage of LC3 blended composites was evaluated in the study done by Li et al. [39]. The authors observed that the autogenous shrinkage curves at early ages showed a steeper slope for Portland Cement samples, and a milder slope for LC3 blended samples. This could be attributed to the slower reaction rate of calcined clay at earlier ages [99]. Additionally, the plateau of the shrinkage strain was reached at later ages with increasing LC3 replacement, possibly due to the slow formation of ettringite, producing a semi-rigid microstructure capable of resisting shrinkage [100]. However, at higher replacement ratios, the matrix was not strong enough to resist

the expansion caused by ettringite. After reaching the plateau stage, increasing LC3 replacement up to 50% resulted in considerable improvement in the autogenous shrinkage (Fig. 12).

Chen et al. [34] measured the drying shrinkage of LC3 pastes up to 90 days and observed that the addition of LC3 resulted in a significant reduction of the drying shrinkage (up to 50%). The finer particle size of calcined clay resulted in significant refinement of the pore size, reducing the amount of capillary pores and in turn, preventing drying out of water from the capillary pores, reducing the drying shrinkage [101], [102].

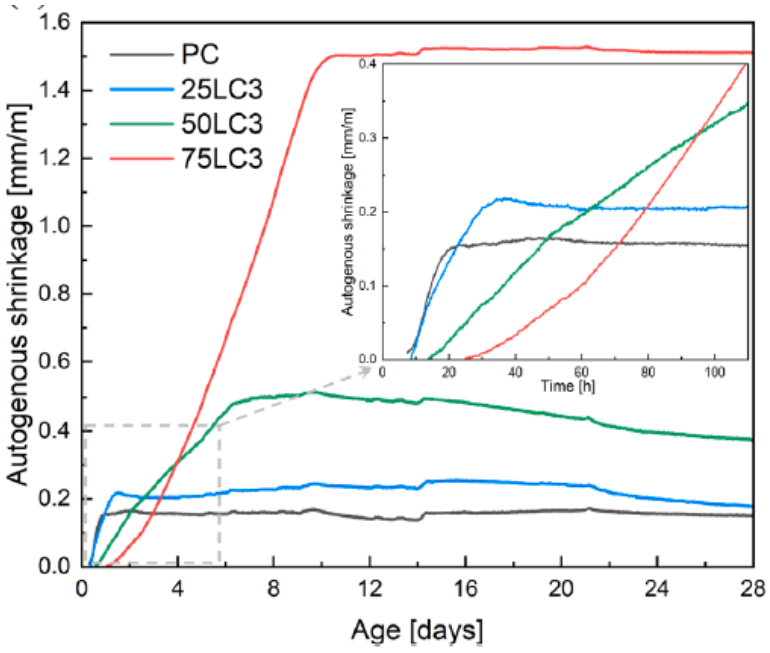

Figure 12. Autogenous shrinkage development up to 28 days, adapted from Ref. [39].

4.6.2 Permeability, Chloride Migration and Accelerated Carbonation

Permeability tests show that PE fiber reinforced LC3 composites showed satisfactory coefficient of permeability in accordance with ASTM 497 [46]. Additionally, the LC3-ECC could be used potentially as a repair liner leading to increase water tightness of structures. Furthermore, PE/PP fiber based ECC retains its self-healing ability and results in reduction of the coefficient of permeability with time [50]. LC3 blended mixes also contributed to lowering the chloride migration coefficients compared to mixed without any replacement, with the average chloride migration coefficient reducing from 1.5 to 0.5 with LC3-50 replacement, at a limestone:clay ratio of 3:1. [45]. The resistance to chloride migration of LC3 blended mixes could be attributed to the refinement of the pore structure of cementitious matrix due to pozzolanic reaction of calcined clay

and the formation of C-A-S-H gel, which can bind chloride ions and increase the resistance to migration [103]. With regards to resistance to carbonation, increasing LC3 content generally resulted in reduced carbonation resistance, as confirmed by accelerated carbonation tests performed by Huang et al. [45] and Luo et al. [43]. This could be explained by the reduced clinker content and the consumption of CH by the calcined clay in the pozzolanic reactions. As a result, the alkalis in the pore solution are reduced, resulting in a lower pH in the pore solution of LC3 composites. Despite the pore refinement of the matrix by the C-A-S-H gel, the overall carbonation resistance was dominated by the reduced content of CH and the pozzolanic reaction consuming CH [45]. However, as carbonation proceeded, the densification of the LC3 pore structure was caused by calcium carbonate precipitated into the macro pores (>0.1 μm) [104], [105]. However, the tests were observed on samples without any fiber incorporation; nonetheless, the pore structure of fiber-reinforced LC3 blends has been observed from microstructural tests.

5 Microstructural Characterization

The hardened properties of the LC3 blended matrices were evaluated by X-ray diffraction (XRD) analysis, thermogravimetric analysis (TGA), mercury intrusion porosimetry (MIP), scanning electron microscopy (SEM), X-ray photoelectron spectroscopy (XPS), micro-computed tomography μCT, nuclear magnetic resonance (NMR) spectroscopy etc. However, not all of the tests are directly related to the behavior of fiber reinforced LC3 composites, since most of the evaluations were done on paste samples, utilizing only binder and water.

A summary of the reaction products and the microstructure of the hardened LC3 matrices is presented in this section. The XRD results revealed that the pozzolanic reaction of calcine clay consumed the portlandite produced by clinker hydration, with higher production of amorphous C-A-S-H gel with increasing LC3 replacement [28], [39]. Incorporation of gypsum and limestone powder resulted in stable ettringite formation, inhibiting the transformation of ettringite to mono-sulfate phases [86], [106]. This ettringite formation may serve as a kind of nano-fiber to improve the tensile ductility and crack toughness of LC3 blends [32]. Limestone particles also react with activated alumina in calcined clay to produce mono-carboaluminates (Mc) and hemi-carboaluminates (Hc), which contribute to the strength of the cementitious matrix [33], [107], [108], [109]. Studies have found that the introduction of seawater into LC3 matrices resulted in the conversion of carboaluminates to Friedel's salts, enhancing the chloride binding capacity of

concrete [47], [107]. Dong et al. [37] reported that higher LC3 replacement resulted in around 62% of mass being amorphous C-A-S-H. It was reported that gypsum is consumed at later ages for LC3 blended mixes, with the calcined clay continuing reaction even after 90 days [43].

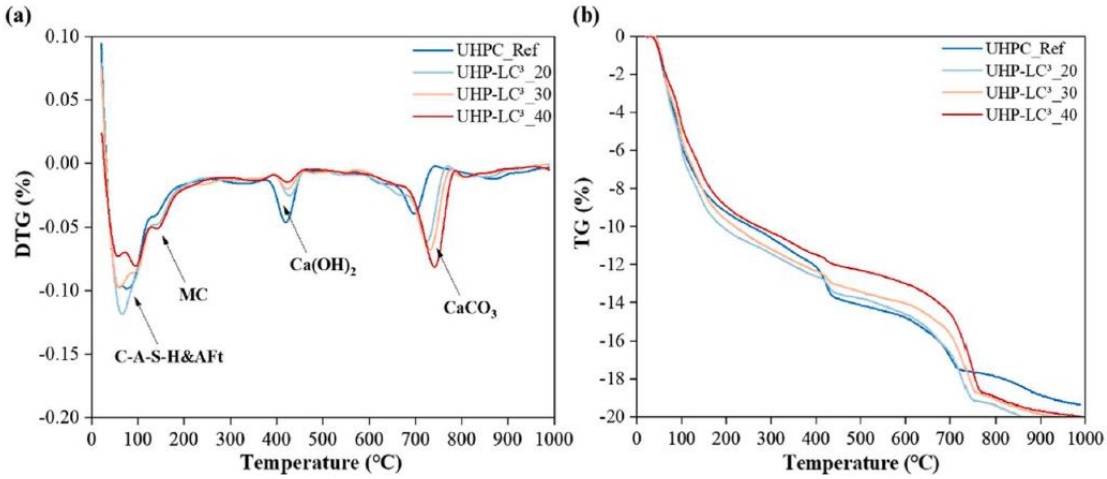

Figure 13: TGA analysis results of LC3 composites, adapted from Ref. [43].

The findings reported from TGA tests further confirmed the microstructure characteristics of LC3 blended mixes. As it can be seen from Fig. 13, the dehydration of water from C-A-S-H gel and ettringite occurs at around 100 °C, mono-carboaluminate is lost at approximately 170 °C, dehydration of portlandite at around 400-500 °C and decomposition of calcite occurs at around 600-800 °C. In some cases, it was found that at high replacement levels, the formation of C-A-S-H via pozzolanic reaction with CH could not fully compensate for the decrease in the amount of hydration products due to lower clinker content [39], [87], which could result in reduced mechanical properties.

Regarding the pore structure of hardened cementitious pastes incorporating LC3, it was found that the early pozzolanic reaction of calcined clay and its filler effect resulted in smaller pore size and less pore volume compared to mixes without LC3 replacement [28], [31], with [39] observing a significant decrease in the mesopores (0.1 µm - 10 µm) due to the hydration of calcined clay. The early strength enhanced by quick pozzolanic reaction to form denser hydration products such as C-A-S-H could be further accelerated by incorporation of SCMs (silica fume, fly-ash, LC3) [34], [43]. It was found that generally, the porosity of hardened pastes improved up to a certain level of LC3 replacement, above which the capillary pores (> 0.1 µm) were seen to increase due to unreacted calcined clay [49]. Due to capillary pores being responsible for micro-crack growth

and propagation, high replacement levels of LC3 will result in a decrease in mechanical strength [110]. At later ages, the C-S-H formed in mixes without LC3 replacement resulted in a significant decrease in the pore size and volume to lower than those incorporating LC3 [28]. At 28 days, it was observed that the pore sizes shifted from 0.01 μm – 0.1 μm to 0.003 μm – 0.01 μm [45], indicating that the pore structure is refined due to the continuous reaction of calcined clay and the formation of ettringite structures and interlayer pores of C-A-S-H gel [111]. However, the overall porosity and the intrudable pores did not correlate entirely with the enhanced mechanical performances of LC3 blends. [38] observed that the volume of harmful decreased regardless of LC3 replacement levels, possibly due to the synergistic effect of nano-SiO_2 in accelerating the hydration reaction of LC3.

At earlier ages, it was observed that increasing fiber content resulted in increased volume of cumulative pores; however, Liu et al. [33] observed that the incorporation of 1.5% PP fiber content resulted in lower pore volume than all other alternatives. Other studies indicate that the addition of 2% PVA will lead to an increase in pores larger than 0.3 μm of more than 3% [111]. Liu et al. [33] postulated that the pores due to increased fiber content could be generated by the interfacial zone between the matrix and the fiber. Conversely, Zhang et al. [52] reported that inclusion of PVA fibers did not result in a significant change in the pore volume of the matrix. Carbon fibers, on the other hand, resulted in a general decreasing trend with increasing fiber reinforcement, with the main reduction in the volume of mesopores (0.1 μm – 10 μm) due to the short carbon fibers with about 7 μm diameter filling the dimensions of several micrometers [39]. However, the volume of gel pores (<0.01 μm) was not influenced by the incorporation of fibers, but the volume of air pores (10 μm-100 μm) slightly increased due to the introduction of air bubbles during mixing. Thus, the size of the fibers and the type of fiber could affect the hardened matrix porosity in different aspects.

From the investigation of the microscopic images (SEM) with energy dispersive x-ray spectroscopy (EDS) of LC3 blended mixes, the presence of Ca and O-rich crystalline particles of $Ca(OH)_2$ surrounded by darker spots of C-S-H gel was observed in mixes without LC3 replacement [33]. From Fig. 14, in LC3 samples, the presence of dense C-A-S-H gel is observed, along with a reduced amount of CH and abundant Al, Si, and O, which indicates the presence of unreacted clay particles in the matrix. The unreacted clay particles are responsible for air pores

which are evident in higher replacement of LC3 mixes from the MIP results and are reflected in the mechanical properties of the matrix as well [43].

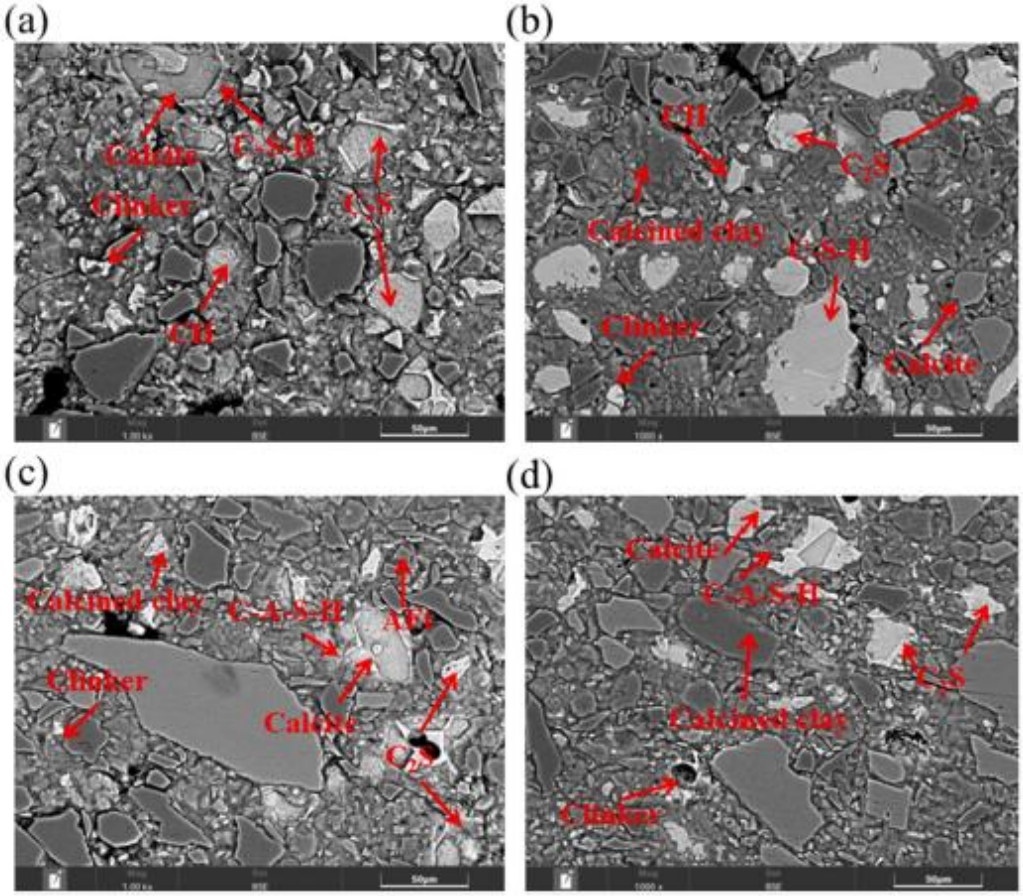

Figure 14. Back-scattered electronic images of LC3 blended UHPC mixes with (a) No replacement, (b) 20%, (c) 30% and (d) 40% replacement, adapted from Ref. [43].

The pozzolanic reaction of LC3 also results in abundant ettringite formation, as confirmed by the TGA and XRD results. Zhou et al. [28] observed that as LC3 content increases, the attached hydration products on PE fibers change from C-S-H gel to ettringite, and at high replacement levels, unreacted $CaCO_3$ can be observed on the fiber surface as well. The presence of ettringite resulting in a deformed shape of PP fibers was noted by Liu et al. [33] as well, resulting in rough interfacial transition zones (ITZ) between the fiber and matrix. Nonetheless, it is also evident that the pores in the ITZ increase with increasing fiber content. (H. Li, Yang, et al., 2023b) also reported that for carbon fibers as well, the LC3 blended matrices produced ettringite on the fiber-matrix interface, resulting in the ettringite crystals expanding the radius of the hole in which the fiber is embedded. The results from ^{29}Si magic angle spinning (MAS) nuclear magnetic resonance (NMR)

spectroscopy revealed the formation of highly polymerized C-A-S-H gel within LC3 blended systems [43], which may result in enhancing the mechanical strength of the matrices [112].

6 Environmental and Economic Aspects

From the environmental impact studies conducted by researchers, it was found that LC3 based binders had low overall environmental impacts despite calcination requiring high temperature and fuel consumption [28]. Also, the calcination and grinding process of LC3 resulted in much higher embodied energy and CO_2 than that of fly-ash [35]. The material sustainability indicators (MSIs) of the main components, namely, energy consumption, CO_2 emissions, and cost for the different fiber reinforced LC3 mixes have been presented in Table 3. The MSIs reported are based on a manufacturing basis from cradle-to-gate, reflecting the sustainability aspects of the different constituents.

Table 3. Cost, CO_2 emission and energy consumption of the components in fiber reinforced LC3 concrete.

Constituent	Cost, USD/t	Energy consumption, GJ/t	CO_2 emission, kg/t
Cement	48 [113]	4.5-6.6 [114]	870-940 [114]
LC3	56.41 [115]	3.99 [116]	550 [115]
Silica Sand	25 [52]	0.226 [52]	33 [52]
Water	1.5 [33]	0 [33]	0 [33]
Superplasticizer	1211 [113]	35 [114]	1667 [114]
PVA fiber	2500-4000 [117]	101 [114]	1710 [113]
PP fiber	1000-2000 [117]	77.24 [118]	3100 [33]
PE fiber	1540-1970 [119]	65-92 [118]	1297-1692 [120]
Steel fiber	800-1500 [117]	30-60 [118]	1600 [121]

It was found that the environmental impact of cement was still the highest among all other components and the constituent fibers ranked only second, although the dosage is quite low [31]. Furthermore, the addition of high range water reducer (HRWR) or superplasticizer due to the high specific surface area of LC3, combined with PE fiber can cause also cause considerable ecological impact in terms of freshwater toxicity aspects [28]. Huang et al. [45] observed that LC3 incorporation could potentially result in nearly 42% decreased carbon emissions and 27% less embodied energy, however, the use of superplasticizers results in a significant source of energy consumption. Gong et al. [31], in their study, reported a 40.31% decrease in global warming potential for a 50% LC3 replacement. From the study done by Zhang et al. [52], it was observed

that although engineering cementitious composites (ECC) result in higher energy consumption, CO_2 emission and higher cost than traditional concrete, utilizing LC3 in ECC resulted in the CO_2 emission being decreased by 31.5%. However, it was still reported that the high use of polymeric fiber resulting in high energy consumption and high costs should be substituted with potential alternatives for advancements in the sustainable development of LC3-ECCs. It was reported by Liu et al. [33] that in the case of PP fibers, the energy consumption increased from 4 GJ/m^3 to 5.65 GJ/m^3 and the CO_2 emissions increased from 267.07 kg/m^3 to 339.69 kg/m^3 with increasing fiber content; conversely, the cost increased by a staggering threefold. Yu et al. [35] experimented with high volume replacement with LC3, incorporating PVA fibers. The results showed that, despite the small dosage, PVA fibers comprised nearly 37% of embodied energy and less than 10% of the total embodied carbon. However, the study [35] did not report the cost analysis of incorporating PVA fibers. However, as observed from Table 3, the PP fiber had a considerable cost advantage over the PVA and PE fibers. Incorporating PP fiber instead of PVA fiber in LC3-ECC can result in energy consumption equal to 55% of PVA based OPC-ECC, and an overall reduction of 61% in material cost and 48% in carbon footprint compared to conventional ECC [50].

LC3 based fiber reinforced concrete can considerably reduce the environmental impacts of typical OPC based fiber reinforced systems. Although some studies [50] observed that the cost of both fiber reinforced LC3 and OPC are similar, generally PE and PP fiber based systems are more economical than PVA fiber based composites. However, the high embodied energy and carbon footprint of fibers and superplasticizers require further research into more sustainable alternatives for producing fiber reinforced concrete.

7 Conclusions

Based on the review conducted on the engineering properties, microstructure characteristics and sustainability aspects of LC3 blended cementitious composites, a few conclusions could be drawn.

1. Utilization of LC3 as a replacement of cement resulted in higher earlier compressive strength, albeit slightly reduced late age strength, compared to only cement mixes. Some researchers also reported higher 28-day compressive strength up to around 30% LC3 replacement.
2. LC3 replacement caused the workability of fresh pastes to decrease and slightly reduce the heat of reduction. The reduced workability is accounted for by utilizing superplasticizers or HRWRA.

3. Incorporating only 2% fiber content resulted in a significant increase in the flexural strength of LC3 blended composites.
4. LC3 blends combined with fiber incorporation resulted in high tensile ductility, toughness, and higher strain capacity compared to conventional concrete, with generally higher LC3 replacement resulting in higher ultimate tensile strain capacity.
5. Although the fiber-matrix interactions could not be explained properly for all fiber types, generally increasing LC3 content resulted in the formation of ettringite on the fiber surface, creating pores in the ITZ, resulting in a reduced fiber-matrix bond. Nonetheless, the bond forces were found to correlate with the ultimate tensile strengths of the matrices.
6. LC3 replacement resulted in a significant decrease in the drying shrinkage, an increase in resistance to chloride migration, and carbonation.
7. Using LC3 as a partial substitution to cement in fiber reinforced concrete resulted in a significant reduction in the global warming potential of the mixes; however, the embodied energy and cost are marginally reduced due to the usage of fibers, admixtures, and the energy-intensive calcination process.
8. Considering the ductility and tensile strain characteristics of fiber-reinforced LC3 over traditional concrete, higher durability and lower maintenance costs can be achieved at a lower construction cost with reduced CO_2 consumption.

Based on the observations from the conducted review, some possible future challenges might exist for construction using fiber reinforced LC3 binders.

1. Properties of clay may vary from region to region, resulting in different behaviors of LC3 blended mixes at a larger scale.
2. The costs and environmental issues regarding fiber incorporation and superplasticizers can scale up when considering real construction, thus further research is be required to optimize the mix design for fiber reinforced LC3 composites. With very few studies found that vary fiber content to different degrees, more effort should be placed on the behavior of fiber reinforced composites at the optimum fiber content.
3. There is a lack of standardized guidelines and acceptance criteria for LC3 based composites. For implementation at a larger scale, more research is required to standardize the characteristics of LC3 blended concrete for different fiber reinforcements.

4. LC3 has the potential to cut down the carbon footprint of the construction industry on a large scale; however, the energy-intensive calcination process should be optimized at the industrial level to further reduce the energy consumption and CO_2 emissions regarding LC3 replacement.
5. Many aspects of the microstructural behavior of fiber reinforced LC3 composites are unexplored and might be somewhat contradictory. Further studies into the microstructural characteristics, particularly at the fiber-matrix interfacial transition zone (ITZ), are required.

References

[1] H. Van Damme, 'Concrete material science: Past, present, and future innovations', *Cem Concr Res*, vol. 112, pp. 5–24, 2018.

[2] K. L. Scrivener, V. M. John, and E. M. Gartner, 'Eco-efficient cements: Potential economically viable solutions for a low-CO2 cement-based materials industry', *Cem Concr Res*, vol. 114, pp. 2–26, 2018.

[3] L. K. Turner and F. G. Collins, 'Carbon dioxide equivalent (CO2-e) emissions: A comparison between geopolymer and OPC cement concrete', *Constr Build Mater*, vol. 43, pp. 125–130, 2013.

[4] L. Wang *et al.*, 'Low-carbon and low-alkalinity stabilization/solidification of high-Pb contaminated soil', *Chemical Engineering Journal*, vol. 351, pp. 418–427, 2018.

[5] H. Li, L. Wang, Y. Zhang, J. Yang, D. C. W. Tsang, and V. Mechtcherine, 'Biochar for sustainable construction industry', in *Current Developments in Biotechnology and Bioengineering*, Elsevier, 2023, pp. 63–95.

[6] J. Yu, D. K. Mishra, C. Hu, C. K. Y. Leung, and S. P. Shah, 'Mechanical, environmental and economic performance of sustainable Grade 45 concrete with ultrahigh-volume Limestone-Calcined Clay (LCC)', *Resour Conserv Recycl*, vol. 175, p. 105846, 2021.

[7] B. Baten, T. Manzur, and I. Ahmed, 'Combined effect of binder type and target mix-design parameters in delaying corrosion initiation time of concrete', *Constr Build Mater*, vol. 242, p. 118003, 2020.

[8] M. Sharma, S. Bishnoi, F. Martirena, and K. Scrivener, 'Limestone calcined clay cement and concrete: A state-of-the-art review', *Cem Concr Res*, vol. 149, p. 106564, 2021.

[9] Y. Tian *et al.*, 'Integrated use of Bayer red mud and electrolytic manganese residue in limestone calcined clay cement (LC3) via thermal treatment activation', *Journal of Building Engineering*, vol. 94, Oct. 2024, doi: 10.1016/j.jobe.2024.109974.

[10] Y. Dhandapani, M. Santhanam, G. Kaladharan, and S. Ramanathan, 'Towards ternary binders involving limestone additions—A review', *Cem Concr Res*, vol. 143, p. 106396, 2021.

[11] Y. Tao, B. P. Gautam, P. M. Pradhan, and C. Hu, 'Characterization and reactivity of Nepali clays as supplementary cementitious material', *Case Studies in Construction Materials*, vol. 16, p. e00947, 2022.

[12] X. Qian *et al.*, 'Sustainable cementitious material with ultra-high content partially calcined limestone-calcined clay', *Constr Build Mater*, vol. 373, p. 130891, 2023.

[13] Y. Dhandapani, T. Sakthivel, M. Santhanam, R. Gettu, and R. G. Pillai, 'Mechanical properties and durability performance of concretes with Limestone Calcined Clay Cement (LC3)', *Cem Concr Res*, vol. 107, pp. 136–151, 2018.

[14] Y. Cao, Y. Wang, Z. Zhang, Y. Ma, and H. Wang, 'Turning sandstone clay into supplementary cementitious material: activation and pozzolanic reactivity evaluation', *Compos B Eng*, vol. 223, p. 109137, 2021.

[15] J. Ambroise, M. Murat, and J. Pera, 'Hydration reaction and hardening of calcined clays and related minerals. IV. Experimental conditions for strength improvement on metakaolinite minicylinders', *Cem Concr Res*, vol. 15, no. 1, pp. 83–88, 1985.

[16] V. L. Bonavetti, V. F. Rahhal, and E. F. Irassar, 'Studies on the carboaluminate formation in limestone filler-blended cements', *Cem Concr Res*, vol. 31, no. 6, pp. 853–859, 2001.

[17] V. Shah, A. Parashar, G. Mishra, S. Medepalli, S. Krishnan, and S. Bishnoi, 'Influence of cement replacement by limestone calcined clay pozzolan on the engineering properties of mortar and concrete', *Advances in Cement Research*, vol. 32, no. 3, pp. 101–111, 2020.

[18] K. Scrivener, F. Martirena, S. Bishnoi, and S. Maity, 'Calcined clay limestone cements (LC3)', *Cem Concr Res*, vol. 114, pp. 49–56, 2018.

[19] S. S. Berriel *et al.*, 'Assessing the environmental and economic potential of Limestone Calcined Clay Cement in Cuba', *J Clean Prod*, vol. 124, pp. 361–369, 2016.

[20] J. Zhang, Q. Luo, and X. Zhang, 'Exploring the influence of calcined clay grade on the rheological dynamics of LC3 mortar', *Constr Build Mater*, vol. 444, Sep. 2024, doi: 10.1016/j.conbuildmat.2024.137852.

[21] A. M. Brandt, 'Fibre reinforced cement-based (FRC) composites after over 40 years of development in building and civil engineering', *Compos Struct*, vol. 86, no. 1–3, pp. 3–9, 2008.

[22] R. F. Zollo, 'Fiber-reinforced concrete: an overview after 30 years of development', *Cem Concr Compos*, vol. 19, no. 2, pp. 107–122, 1997.

[23] G. Choe, G. Kim, H. Kim, E. Hwang, S. Lee, and J. Nam, 'Effect of amorphous metallic fiber on mechanical properties of high-strength concrete exposed to high-temperature', *Constr Build Mater*, vol. 218, pp. 448–456, 2019.

[24] M. G. Alberti, A. Enfedaque, and J. C. Gálvez, 'On the mechanical properties and fracture behavior of polyolefin fiber-reinforced self-compacting concrete', *Constr Build Mater*, vol. 55, pp. 274–288, 2014.

[25] R. M. De Gutiérrez, L. N. Diaz, and S. Delvasto, 'Effect of pozzolans on the performance of fiber-reinforced mortars', *Cem Concr Compos*, vol. 27, no. 5, pp. 593–598, 2005.

[26] B.-T. Huang, J.-Q. Wu, J. Yu, J.-G. Dai, C. K. Y. Leung, and V. C. Li, 'Seawater sea-sand engineered/strain-hardening cementitious composites (ECC/SHCC): Assessment and modeling of crack characteristics', *Cem Concr Res*, vol. 140, p. 106292, 2021, doi: https://doi.org/10.1016/j.cemconres.2020.106292.

[27] D. Zhang, W. Wang, and V. C. Li, 'Microcrack characterization of loaded Engineered Cementitious Composites via optical scans and photogrammetric analyses', *Constr Build Mater*, vol. 318, p. 126000, 2022.

[28] Y. Zhou, G. Gong, B. Xi, M. Guo, F. Xing, and C. Chen, 'Sustainable lightweight engineered cementitious composites using limestone calcined clay cement (LC3)', *Compos B Eng*, vol. 243, p. 110183, 2022, doi: https://doi.org/10.1016/j.compositesb.2022.110183.

[29] B. A. Graybeal, 'Material property characterization of ultra-high performance concrete', United States. Federal Highway Administration. Office of Infrastructure …, 2006.

[30] A. Korpa, T. Kowald, and R. Trettin, 'Phase development in normal and ultra high performance cementitious systems by quantitative X-ray analysis and thermoanalytical methods', *Cem Concr Res*, vol. 39, no. 2, pp. 69–76, 2009.

[31] G. Gong *et al.*, 'Multiscale Investigation on the Performance of Engineered Cementitious Composites Incorporating PE Fiber and Limstone Calcined Clay Cement (LC3)', *Polymers (Basel)*, vol. 14, no. 7, Apr. 2022, doi: 10.3390/polym14071291.

[32] L. Wang *et al.*, 'On the use of limestone calcined clay cement (LC3) in high-strength strain-hardening cement-based composites (HS-SHCC)', *Cem Concr Res*, vol. 144, Jun. 2021, doi: 10.1016/j.cemconres.2021.106421.

[33] J. Liu, W. Zhang, Z. Li, H. Jin, and L. Tang, 'Mechanics, hydration phase and pore development of embodied energy and carbon composites based on ultrahigh-volume low-carbon cement with limestone calcined clay', *Case Studies in Construction Materials*, vol. 17, p. e01299, 2022.

[34] W. Chen, H. Zhu, Y. Li, L. Yang, S. Cheng, and H. Yu, 'Engineered cementitious composites using blended limestone calcined clay and fly ash: Mechanical properties and drying shrinkage modeling', *Case Studies in Construction Materials*, p. e02960, 2024.

[35] J. Yu, H. L. Wu, and C. K. Y. Leung, 'Feasibility of using ultrahigh-volume limestone-calcined clay blend to develop sustainable medium-strength Engineered Cementitious Composites (ECC)', *J Clean Prod*, vol. 262, Jul. 2020, doi: 10.1016/j.jclepro.2020.121343.

[36] D. Guo, M. Guo, F. Xing, Y. Zhou, Z. Huang, and W. Cao, 'Using limestone calcined clay cement and recycled fine aggregate to make ultra-high-performance concrete: Properties and environmental impact', *Constr Build Mater*, vol. 394, p. 132026, 2023, doi: https://doi.org/10.1016/j.conbuildmat.2023.132026.

[37] Y. Dong, Y. Liu, and C. Hu, 'Towards greener ultra-high performance concrete based on highly-efficient utilization of calcined clay and limestone powder', *Journal of Building Engineering*, vol. 66, p. 105836, 2023.

[38] D. Guo, M. Guo, Y. Zhou, and Z. Zhu, 'Use of nano-silica to improve the performance of LC3-UHPC: Mechanical behavior and microstructural characteristics', *Constr Build Mater*, vol. 411, Jan. 2024, doi: 10.1016/j.conbuildmat.2023.134280.

[39] H. Li *et al.*, 'Multiscale assessment of performance of limestone calcined clay cement (LC3) reinforced with virgin and recycled carbon fibers', *Constr Build Mater*, vol. 406, Nov. 2023, doi: 10.1016/j.conbuildmat.2023.133228.

[40] B. Zhu, J. Pan, B. Nematollahi, Z. Zhou, Y. Zhang, and J. Sanjayan, 'Development of 3D printable engineered cementitious composites with ultra-high tensile ductility for digital construction', *Mater Des*, vol. 181, p. 108088, 2019, doi: https://doi.org/10.1016/j.matdes.2019.108088.

[41] K. A. Ibrahim, G. P. A. G. van Zijl, and A. J. Babafemi, 'Comparative studies of LC3- and fly ash-based blended binders in fibre-reinforced printed concrete (FRPC): Rheological and quasi-static mechanical characteristics', *Journal of Building Engineering*, vol. 80, Dec. 2023, doi: 10.1016/j.jobe.2023.108016.

[42] A. Al-Fakih, M. A. Al-Shugaa, M. A. Al-Osta, and B. S. Thomas, 'Mechanical, environmental, and economic performance of engineered cementitious composite incorporated limestone calcined clay cement: A review', Nov. 15, 2023, *Elsevier Ltd*. doi: 10.1016/j.jobe.2023.107901.

[43] Q. Luo, X. Zhang, Y. Bai, J. Yang, and G. Geng, 'Reduce the cost and embodied carbon of ultrahigh performance concrete using waste clay', *Case Studies in Construction Materials*, vol. 19, p. e02670, 2023.

[44] C. Signorini *et al.*, 'Assessing the stress-transfer capability of mineral impregnated PBO yarns in a limestone calcined clay cement-based (LC3) matrix', *Compos B Eng*, vol. 276, p. 111364, 2024.

[45] Z. HUANG, T. LIANG, and C. Lijie, 'Experimental studies on durability performances of ultra-lightweight low-carbon LC3 cement composites against chloride ingression and carbonation', *Constr Build Mater*, vol. 395, p. 132340, 2023.

[46] H. Zhu, T. Wang, Y. Wang, W.-H. Hu, and V. C. Li, 'Feasibility of structural retrofit concrete pipelines using limestone calcined clay cement Engineered Cementitious Composites (LC3 ECC)', *Eng Struct*, vol. 289, p. 116305, 2023.

[47] Q. Zhou, Y. Zhou, Z. Guan, F. Xing, M. Guo, and B. Hu, 'Mechanical Performance and Constitutive Model Analysis of Concrete Using PE Fiber-Strengthened Recycled Coarse Aggregate', *Polymers (Basel)*, vol. 14, no. 19, Oct. 2022, doi: 10.3390/polym14193964.

[48] M. Mohammadi *et al.*, 'Interfacial properties of high-strength, limestone-calcined clay cement (LC3) matrix and PE fibers, surface-modified using dopamine and tannic acid', *Constr Build Mater*, vol. 408, p. 133537, 2023.

[49] L. Wang, Z. Zhu, A. Hamza Ahmed, M. Liebscher, X. Zhu, and V. Mechtcherine, 'Self-healing behavior of high-strength strain-hardening cement-based composites (HS-SHCC) blended with limestone calcined clay cement (LC3)', *Constr Build Mater*, vol. 370, Mar. 2023, doi: 10.1016/j.conbuildmat.2023.130633.

[50] H. Zhu, D. Zhang, T. Wang, H. Wu, and V. C. Li, 'Mechanical and self-healing behavior of low carbon engineered cementitious composites reinforced with PP-fibers', *Constr Build Mater*, vol. 259, p. 119805, 2020, doi: https://doi.org/10.1016/j.conbuildmat.2020.119805.

[51] H. Zhu, K. Yu, and V. C. Li, 'Sprayable engineered cementitious composites (ECC) using calcined clay limestone cement (LC3) and PP fiber', *Cem Concr Compos*, vol. 115, p. 103868, 2021.

[52] D. Zhang, B. Jaworska, H. Zhu, K. Dahlquist, and V. C. Li, 'Engineered Cementitious Composites (ECC) with limestone calcined clay cement (LC3)', *Cem Concr Compos*, vol. 114, p. 103766, 2020.

[53] V. Afroughsabet, L. Biolzi, and T. Ozbakkaloglu, 'High-performance fiber-reinforced concrete: a review', *J Mater Sci*, vol. 51, no. 14, pp. 6517–6551, 2016, doi: 10.1007/s10853-016-9917-4.

[54] C. Zhao, Z. Wang, Z. Zhu, Q. Guo, X. Wu, and R. Zhao, 'Research on different types of fiber reinforced concrete in recent years: An overview', *Constr Build Mater*, vol. 365, p. 130075, 2023, doi: https://doi.org/10.1016/j.conbuildmat.2022.130075.

[55] A. K. Das and C. K. Y. Leung, 'The Use of Ultra-high Volume of Lime Stone Calcine Clay to Produce Basalt Fiber Reinforced Strain Hardening Cementitious Composites', in *International Conference on Strain-Hardening Cement-Based Composites*, Springer, 2022, pp. 13–22.

[56] W. Liu *et al.*, 'Chapter Two - Radiation Technology Application in High-Performance Fibers and Functional Textiles', in *Radiation Technology for Advanced Materials*, G. Wu, M. Zhai, and M. Wang, Eds., Academic Press, 2019, pp. 13–73. doi: https://doi.org/10.1016/B978-0-12-814017-8.00002-0.

[57] Z. Lin and V. C. Li, 'Crack bridging in fiber reinforced cementitious composites with slip-hardening interfaces', *J Mech Phys Solids*, vol. 45, no. 5, pp. 763–787, 1997, doi: https://doi.org/10.1016/S0022-5096(96)00095-6.

[58] K. Yu, L. Li, J. Yu, Y. Wang, J. Ye, and Q. Xu, 'Direct tensile properties of engineered cementitious composites: A review', *Constr Build Mater*, vol. 165, pp. 346–362, 2018, doi: https://doi.org/10.1016/j.conbuildmat.2017.12.124.

[59] Y. Jiangtao, Y. Junhong, Z. Bin, X. Shilang, W. Bin, and Y. Kequan, 'Dynamic Response of Concrete Frames Including Plain Ductile Cementitious Composites', *Journal of Structural Engineering*, vol. 145, no. 6, p. 04019042, Jun. 2019, doi: 10.1061/(ASCE)ST.1943-541X.0002292.

[60] F. Dong, J. Yu, K. Zhan, and Z. Li, 'Seismic fragility analysis of two-story ultra-high ductile cementitious composites frame without steel reinforcement', *Advances in Structural Engineering*, vol. 23, no. 11, pp. 2373–2387, Apr. 2020, doi: 10.1177/1369433220912350.

[61] British Standards Institution., *Fibres for concrete. Part 2, Polymer fibres - definitions, specifications and conformity*.

[62] J. Blazy and R. Blazy, 'Polypropylene fiber reinforced concrete and its application in creating architectural forms of public spaces', *Case Studies in Construction Materials*, vol. 14, p. e00549, 2021, doi: https://doi.org/10.1016/j.cscm.2021.e00549.

[63] S. Yin, R. Tuladhar, F. Shi, M. Combe, T. Collister, and N. Sivakugan, 'Use of macro plastic fibres in concrete: A review', *Constr Build Mater*, vol. 93, pp. 180–188, 2015, doi: https://doi.org/10.1016/j.conbuildmat.2015.05.105.

[64] M. Ozawa, S. Subedi Parajuli, Y. Uchida, and B. Zhou, 'Preventive effects of polypropylene and jute fibers on spalling of UHPC at high temperatures in combination with waste porous ceramic fine aggregate as an internal curing material', *Constr Build Mater*, vol. 206, pp. 219–225, 2019, doi: https://doi.org/10.1016/j.conbuildmat.2019.02.056.

[65] O. Gencel, C. Ozel, W. Brostow, and G. Martínez-Barrera, 'Mechanical properties of self-compacting concrete reinforced with polypropylene fibres', *Materials Research Innovations*, vol. 15, no. 3, pp. 216–225, Jun. 2011, doi: 10.1179/143307511X13018917925900.

[66] Z. H. Mahdi, B. H. Maula, A. S. Ali, and M. R. Abdulghani, 'Influence of Sand Size on Mechanical Properties of Fiber Reinforced Polymer Concrete', vol. 9, no. 1, pp. 554–560, 2019, doi: doi:10.1515/eng-2019-0066.

[67] J. Wang, Q. Dai, R. Si, and S. Guo, 'Investigation of properties and performances of Polyvinyl Alcohol (PVA) fiber-reinforced rubber concrete', *Constr Build Mater*, vol. 193, pp. 631–642, 2018.

[68] A. Noushini, K. Vessalas, and B. Samali, 'Static mechanical properties of polyvinyl alcohol fibre reinforced concrete (PVA-FRC)', *Magazine of Concrete Research*, vol. 66, no. 9, pp. 465–483, 2014.

[69] S.-H. Xiao *et al.*, 'Dynamic properties of PVA short fiber reinforced low-calcium fly ash-slag geopolymer under an SHPB impact load', *Journal of Building Engineering*, vol. 44, p. 103220, 2021.

[70] C. Zhao, Z. Wang, Z. Zhu, Q. Guo, X. Wu, and R. Zhao, 'Research on different types of fiber reinforced concrete in recent years: An overview', *Constr Build Mater*, vol. 365, p. 130075, 2023, doi: https://doi.org/10.1016/j.conbuildmat.2022.130075.

[71] A. Balea, E. Fuente, M. C. Monte, Á. Blanco, and C. Negro, '20 - Fiber reinforced cement based composites', in *Fiber Reinforced Composites*, K. Joseph, K. Oksman, G. George, R. Wilson, and S.

Appukuttan, Eds., Woodhead Publishing, 2021, pp. 597–648. doi: https://doi.org/10.1016/B978-0-12-821090-1.00019-3.

[72] T. Tahenni, F. Bouziadi, B. Boulekbache, and S. Amziane, 'Experimental and numerical investigation of the effect of steel fibres on the deflection behaviour of reinforced concrete beams without stirrups', *Structures*, vol. 33, pp. 1603–1619, 2021, doi: https://doi.org/10.1016/j.istruc.2021.05.005.

[73] C. P. Kumar and M. S. Hameed, 'Experimental study on the behaviour of steel fibre when used as a secondary reinforcement in reinforced concrete beam', *Mater Today Proc*, vol. 52, pp. 1189–1196, 2022.

[74] J. Ran, T. Li, D. Chen, L. Shang, W. Li, and Q. Zhu, 'Mechanical properties of concrete reinforced with corrugated steel fiber under uniaxial compression and tension', *Structures*, vol. 34, pp. 1890–1902, 2021, doi: https://doi.org/10.1016/j.istruc.2021.08.135.

[75] P. Davies, A. R. Bunsell, and E. Chailleux, 'Tensile fatigue behaviour of PBO fibres', *J Mater Sci*, vol. 45, no. 23, pp. 6395–6400, 2010, doi: 10.1007/s10853-010-4721-z.

[76] I. Curosu *et al.*, 'Influence of fiber type on the tensile behavior of high-strength strain-hardening cement-based composites (SHCC) at elevated temperatures', *Mater Des*, vol. 198, p. 109397, 2021, doi: https://doi.org/10.1016/j.matdes.2020.109397.

[77] T. Trapko, K. Rogalski, M. Musiał, and L. Ombres, 'Effectiveness of Concrete Elements Strengthening through PBO-FRCM Confinement with Various Types of Anchorage', *Journal of Materials in Civil Engineering*, vol. 33, no. 1, p. 04020409, 2021.

[78] I. Curosu, M. Liebscher, V. Mechtcherine, C. Bellmann, and S. Michel, 'Tensile behavior of high-strength strain-hardening cement-based composites (HS-SHCC) made with high-performance polyethylene, aramid and PBO fibers', *Cem Concr Res*, vol. 98, pp. 71–81, 2017, doi: https://doi.org/10.1016/j.cemconres.2017.04.004.

[79] H. Tanyildizi, 'Effect of temperature, carbon fibers, and silica fume on the mechanical properties of lightweight concretes', *Carbon N Y*, vol. 47, no. 6, pp. 1614–1615, 2009, doi: https://doi.org/10.1016/j.carbon.2008.12.013.

[80] M. Rutzen and D. Volkmer, 'Viscoelasticity and energy dissipation as indicators of flexural fatigue behavior in a ductile carbon fiber-reinforced cementitious composite', *Int J Fatigue*, vol. 160, p. 106839, 2022.

[81] M. Nagi and J.-W. Hsu, 'Optimization of the use of lightweight aggregates in carbon fiber reinforced cement', *Materials Journal*, vol. 89, no. 3, pp. 267–276, 1992.

[82] S. Liu, Y. Ge, M. Wu, H. Xiao, and Y. Kong, 'Properties and road engineering application of carbon fiber modified-electrically conductive concrete', *Structural Concrete*, vol. 22, no. 1, pp. 410–421, Feb. 2021, doi: https://doi.org/10.1002/suco.201900510.

[83] Y. Briki, M. Zajac, M. Ben Haha, and K. Scrivener, 'Impact of limestone fineness on cement hydration at early age', *Cem Concr Res*, vol. 147, p. 106515, 2021.

[84] F. Avet and K. Scrivener, 'Investigation of the calcined kaolinite content on the hydration of Limestone Calcined Clay Cement (LC3)', *Cem Concr Res*, vol. 107, pp. 124–135, 2018.

[85] F. Zunino and K. Scrivener, 'Insights on the role of alumina content and the filler effect on the sulfate requirement of PC and blended cements', *Cem Concr Res*, vol. 160, p. 106929, 2022, doi: https://doi.org/10.1016/j.cemconres.2022.106929.

[86] F. Zunino and K. Scrivener, 'Factors influencing the sulfate balance in pure phase C3S/C3A systems', *Cem Concr Res*, vol. 133, p. 106085, 2020, doi: https://doi.org/10.1016/j.cemconres.2020.106085.

[87] Z. Zhang, F. Yang, J.-C. Liu, and S. Wang, 'Eco-friendly high strength, high ductility engineered cementitious composites (ECC) with substitution of fly ash by rice husk ash', *Cem Concr Res*, vol. 137, p. 106200, 2020.

[88] W. Zhang *et al.*, 'Investigation on mechanical properties improvement of seawater engineered cementitious composites (ECC) using FA/LC2', *Constr Build Mater*, vol. 345, Aug. 2022, doi: 10.1016/j.conbuildmat.2022.128271.

[89] H. Nguyen *et al.*, 'Ettringite-based binder from ladle slag and gypsum – The effect of citric acid on fresh and hardened state properties', *Cem Concr Res*, vol. 123, p. 105800, 2019, doi: https://doi.org/10.1016/j.cemconres.2019.105800.

[90] P. Duan, Z. Shui, W. Chen, and C. Shen, 'Effects of metakaolin, silica fume and slag on pore structure, interfacial transition zone and compressive strength of concrete', *Constr Build Mater*, vol. 44, pp. 1–6, 2013, doi: https://doi.org/10.1016/j.conbuildmat.2013.02.075.

[91] G. A. Arce, H. Noorvand, M. M. Hassan, T. Rupnow, and N. Dhakal, 'Feasibility of low fiber content PVA-ECC for jointless pavement application', *Constr Build Mater*, vol. 268, p. 121131, 2021.

[92] H. Yokota, K. Rokugo, and N. Sakata, 'Recommendations for Design and Construction of High Performance Fiber Reinforced Cement Composite with Multiple Fine Cracks', 2007. [Online]. Available: https://api.semanticscholar.org/CorpusID:195738266

[93] G. P. A. G. van Zijl, V. Slowik, R. D. Toledo Filho, F. H. Wittmann, and H. Mihashi, 'Comparative testing of crack formation in strain-hardening cement-based composites (SHCC)', *Mater Struct*, vol. 49, pp. 1175–1189, 2016.

[94] V. C. Li, *Engineered cementitious composites (ECC): bendable concrete for sustainable and resilient infrastructure*. Springer, 2019.

[95] F. N. Santos, S. R. G. de Sousa, A. J. F. Bombard, and S. L. Vieira, 'Rheological study of cement paste with metakaolin and/or limestone filler using mixture design of experiments', *Constr Build Mater*, vol. 143, pp. 92–103, 2017.

[96] M. Butler, V. Mechtcherine, and S. Hempel, 'Experimental investigations on the durability of fibre–matrix interfaces in textile-reinforced concrete', *Cem Concr Compos*, vol. 31, no. 4, pp. 221–231, 2009.

[97] D. B. Marshall, B. N. Cox, and A. G. Evans, 'The mechanics of matrix cracking in brittle-matrix fiber composites', *Acta metallurgica*, vol. 33, no. 11, pp. 2013–2021, 1985.

[98] S. Chen, Y. Xie, T. Xiao, W. Zhao, J. Li, and C. Zhao, 'Tannic acid-inspiration and post-crosslinking of zwitterionic polymer as a universal approach towards antifouling surface', *Chemical Engineering Journal*, vol. 337, pp. 122–132, 2018.

[99] Y. Zhao and Y. Zhang, 'A review on hydration process and setting time of limestone calcined clay cement (LC3)', *Solids*, vol. 4, no. 1, pp. 24–38, 2023.

[100] R. Hay, L. Li, and K. Celik, 'Shrinkage, hydration, and strength development of limestone calcined clay cement (LC3) with different sulfation levels', *Cem Concr Compos*, vol. 127, p. 104403, 2022, doi: https://doi.org/10.1016/j.cemconcomp.2021.104403.

[101] A. Dixit, H. Du, J. Dang, and S. Dai Pang, 'Quaternary blended limestone-calcined clay cement concrete incorporating fly ash', *Cem Concr Compos*, vol. 123, p. 104174, 2021.

[102] S. Afroz, Y. Zhang, Q. D. Nguyen, T. Kim, and A. Castel, 'Shrinkage of blended cement concrete with fly ash or limestone calcined clay', *Mater Struct*, vol. 56, no. 1, p. 15, 2023, doi: 10.1617/s11527-023-02099-8.

[103] R. Neves, F. Branco, and J. De Brito, 'Field assessment of the relationship between natural and accelerated concrete carbonation resistance', *Cem Concr Compos*, vol. 41, pp. 9–15, 2013.

[104] J. Liu, X. Fan, J. Liu, H. Jin, J. Zhu, and W. Liu, 'Investigation on mechanical and micro properties of concrete incorporating seawater and sea sand in carbonized environment', *Constr Build Mater*, vol. 307, p. 124986, 2021.

[105] B. Wu and G. Ye, 'Development of porosity of cement paste blended with supplementary cementitious materials after carbonation', *Constr Build Mater*, vol. 145, pp. 52–61, 2017.

[106] S. Krishnan, A. C. Emmanuel, and S. Bishnoi, 'Hydration and phase assemblage of ternary cements with calcined clay and limestone', *Constr Build Mater*, vol. 222, pp. 64–72, 2019.

[107] M. Zajac, A. Rossberg, G. Le Saout, and B. Lothenbach, 'Influence of limestone and anhydrite on the hydration of Portland cements', *Cem Concr Compos*, vol. 46, pp. 99–108, 2014, doi: https://doi.org/10.1016/j.cemconcomp.2013.11.007.

[108] B. Lothenbach, G. Le Saout, E. Gallucci, and K. Scrivener, 'Influence of limestone on the hydration of Portland cements', *Cem Concr Res*, vol. 38, no. 6, pp. 848–860, 2008, doi: https://doi.org/10.1016/j.cemconres.2008.01.002.

[109] T. Matschei, B. Lothenbach, and F. P. Glasser, 'The role of calcium carbonate in cement hydration', *Cem Concr Res*, vol. 37, no. 4, pp. 551–558, 2007, doi: https://doi.org/10.1016/j.cemconres.2006.10.013.

[110] L. Wang *et al.*, 'The roles of biochar as green admixture for sediment-based construction products', *Cem Concr Compos*, vol. 104, p. 103348, 2019, doi: https://doi.org/10.1016/j.cemconcomp.2019.103348.

[111] Y. Shen, Q. Li, B. Huang, X. Liu, and S. Xu, 'Effects of PVA fibers on microstructures and hydration products of cementitious composites with and without fly ash', *Constr Build Mater*, vol. 360, p. 129533, 2022, doi: https://doi.org/10.1016/j.conbuildmat.2022.129533.

[112] A. Rafeet, R. Vinai, M. Soutsos, and W. Sha, 'Effects of slag substitution on physical and mechanical properties of fly ash-based alkali activated binders (AABs)', *Cem Concr Res*, vol. 122, pp. 118–135, 2019.

[113] H.-L. Wu, D. Zhang, B. R. Ellis, and V. C. Li, 'Development of reactive MgO-based Engineered Cementitious Composite (ECC) through accelerated carbonation curing', *Constr Build Mater*, vol. 191, pp. 23–31, 2018, doi: https://doi.org/10.1016/j.conbuildmat.2018.09.196.

[114] F. Pacheco-Torgal, Z. Abdollahnejad, S. Miraldo, and M. Kheradmand, 'Chapter 9 - Alkali-Activated Cement-Based Binders (AACBs) as Durable and Cost-Competitive Low-CO2 Binder Materials: Some Shortcomings That Need to be Addressed', in *Handbook of Low Carbon Concrete*, A. Nazari and J. G. Sanjayan, Eds., Butterworth-Heinemann, 2017, pp. 195–216. doi: https://doi.org/10.1016/B978-0-12-804524-4.00009-9.

[115] S. Sánchez Berriel *et al.*, 'Assessing the environmental and economic potential of Limestone Calcined Clay Cement in Cuba', *J Clean Prod*, vol. 124, pp. 361–369, 2016, doi: https://doi.org/10.1016/j.jclepro.2016.02.125.

[116] R. Gettu *et al.*, 'Influence of supplementary cementitious materials on the sustainability parameters of cements and concretes in the Indian context', *Mater Struct*, vol. 52, no. 1, p. 10, 2019, doi: 10.1617/s11527-019-1321-5.

[117] R. Jabbour, J. J. Assaad, and B. Hamad, 'Cost-to-performance assessment of polyvinyl alcohol fibers in concrete structures', *Mechanics of Advanced Materials and Structures*, vol. 29, no. 20, pp. 2973–2983, 2022, doi: 10.1080/15376494.2021.1882625.

[118] Y. S. Song, J. R. Youn, and T. G. Gutowski, 'Life cycle energy analysis of fiber-reinforced composites', *Compos Part A Appl Sci Manuf*, vol. 40, no. 8, pp. 1257–1265, 2009, doi: https://doi.org/10.1016/j.compositesa.2009.05.020.

[119] T. Röding, J. Langer, T. Modenesi Barbosa, M. Bouhrara, and T. Gries, 'A review of polyethylene-based carbon fiber manufacturing', *Applied Research*, vol. 1, no. 3, p. e202100013, Oct. 2022, doi: https://doi.org/10.1002/appl.202100013.

[120] P. T. Benavides, U. Lee, and O. Zarè-Mehrjerdi, 'Life cycle greenhouse gas emissions and energy use of polylactic acid, bio-derived polyethylene, and fossil-derived polyethylene', *J Clean Prod*, vol. 277, Dec. 2020, doi: 10.1016/j.jclepro.2020.124010.

[121] I. M. Nikbin *et al.*, 'Life cycle assessment and mechanical properties of high strength steel fiber reinforced concrete containing waste PET bottle', *Constr Build Mater*, vol. 337, p. 127553, 2022, doi: https://doi.org/10.1016/j.conbuildmat.2022.127553.